Study of RIP1/RIP3 Peptides Aggregation In Vitro

by

Maytham G Ismail

A thesis submitted in partial fulfillment
of the requirements for the degree of
Master of Science in Engineering
(Mechanical Engineering)
in the University of Michigan-Dearborn
2021

Master's Thesis Committee:

Associate Professor Mathumai Kanapathipillai, Chair
Associate Professor Gargi Ghosh
Associate Professor Joe Lo

Acknowledgements

First, I would like to acknowledge and give my warmest thanks from my deepest heart to my advisor, Dr. Mathumai Kanapathipillai, who made this work possible. Her continuous support, guidance, advice, enthusiasm, motivation, and patience carried me through all the stages of my research. Also, I would like to thank the University of Michigan Dearborn department of Mechanical engineering for the laboratory environment to finish my experiments. Also, I would like to thank my committee members Dr. Joe Lo, and Dr. Gargi Ghosh for letting my defense be an enjoyable moment, and for their comments and suggestions, thanks to you.

In addition, I would like to give special thanks to my wife Zahraa Maadal for her support and encouragement.

Finally, I would like to thank my family especially my father and my mother for their continuous love, care, and inspiration.

Table of Contents

List of Tables

List of Figures

List of Abbreviations

CPZ	Chlorpromazine Hydrochloride
DD	Death Domain
DLS	Dynamic Light Scattering
DMEM	Dulbecco's Modified Eagle Medium
DMSO	Dimethyl Sulfoxide
FITC	Fluorescein Isothiocyanate
IQIG	Isoleucine/Glutamine/Isoleucine/Glycine
KD	Kinase Domain
MLKL	Mixed Lineage Kinase Domain Like
MOPS	(3-(N-morpholino) propanesulfonic acid)
NH4OAC	Ammonium Acetate
PQC	Protein Quality Control
RHIM	RIP Homotypic Interaction Motif
RIPK1	Receptor Interacting Serine/Threonine Protein Kinase1
RIPK3	Receptor Interacting Serine/Threonine Protein Kinase3
TEM	Transmission Electron Microscopy
ThT	Thioflavin T
TNF-α	Tumor Necrosis Factor alpha
TRAIL	TNF-Related Apoptosis Inducing Ligand
VQVG	Valine/Glutamine/Valine/Glycine

Abstract

This master's thesis study investigates RIP1/RIP3 peptide aggregation In Vitro. Protein aggregates play a major role in diseases and in normal physiological function. Although several studies have been done on the disease-causing protein and peptide aggregates, not much have been investigated on protein aggregates that play a role in normal physiological processes. Examples of protein aggregation in normal cellular function are the receptor interacting protein kinases 1 and 3, as well as RIP1/RIP3 aggregates complexes in cellular necroptosis. RIP1/RIP3 proteins form a protein aggregate complex during necroptosis. Although there are some studies on full kinase proteins aggregation, little has been done to investigate the potential of small peptide sequences of RIP1/RIP3 proteins on their aggregation mechanism, physicochemical properties, cellular functions, and potential biomedical applications. In this thesis, we study peptides consisting of four and twelve amino acid sequences of RIP1/ RIP3 proteins that are known to drive the beta-sheet formation and play a major role in the aggregation. The study was aided by biochemical, biophysical, mechanical, microscopy characterization, and cellular assays. The thesis study revealed that the 12 amino acid peptides exhibited amyloid like aggregates properties, and also showed mechano sensitive properties. Further, the aggregates induced cellular necrosis compared to apoptosis. The thesis study would aid in further studies on RIP1/RIP3 peptide and protein aggregation, which could be useful in understanding their role in multiple cellular functions and diseases.

Chapter 1 : Introduction

1.1. Introduction

Protein aggregates are misfolded proteins adopt a conformation that cause its polymerization into aggregates and organized fibrils [1]. This aggregation transforms the normal form of protein into the misfolded form, which involves a transition of alpha-helical structure elements into beta-sheet. Protein aggregation plays a key role in pathological and normal physiological process [2]. Hence, protein aggregation is a major topic of interest in the fields of protein research and clinical medicine.

Among the protein aggregation processes relevant to normal physiological process, amyloid complex formed by receptor interacting protein (RIP) kinases is one of the key examples. It has been reported that RIP1/RIP3 proteins form amyloid-like signaling complex that is essential for the necroptosis process [4]. Receptor interacting protein RIP kinases contain seven members, all have a kinase domain (KD), and are important regulators of cell death and survival [3]. Receptor interacting protein kinase 1/3 play a key role as signaling molecules in necroptosis, which is programmed necrosis (a pathway of cell death) [4]. RIP1 contains a C-terminal death domain, where RIP1 can engage to signal complexes that initiate different pathways. RIP3 has a C-terminus that is varied from any other recognized proteins. However, a RIP homotypic interaction motif (RHIM) found in the intermediate domain of RIP1 was also identified in the C-terminus of RIP3. The RHIM domain is likely to mediate protein–protein interactions, because it is required for the interaction between RIP3 and RIP1. (Figure 1.1) depicts the structural

diagrams of RIP1 and RIP3 [4]. Recently, studies have been reported on the amyloid formation for RIP1/RIP3. Studies have shown that RIP1/RIP3 form amyloid like structures in vitro [5,6,7]. Further studies report that the RHIM (RIP homotypic interaction motifs) of the RIP1 and RIP3 proteins are responsible for the amyloid like filamentous structure [6,7]. The core region contains sequences IQIG and VQVG of the RIP1 and RIP3 proteins RHIM regions respectively and is assumed that the Ile and Val amino acid residues form the double beta sheet structure [6,7]. Although studies have reported the role of full RIP1/RIP3 protein aggregates, detailed study of the protein aggregates and their effects, studies on short peptide sequences and their potential application as drug depot have not been studied yet, and hence is the motivation of this thesis. Short peptide sequences consisting of the core region of the RIP1 and RIP3 proteins that would form aggregates are chosen for studying the aggregation mechanism and applications due to their relatively easier handling and lower cost.

The thesis involves the study of small peptides of RIP1 and RIP3 protein aggregation in vitro. The sequences are IQIG, TIYNSTGIQIGA, of RIP1-4 short and RIP1-12 long, and VQVG, NIYNCSGVQVGD of RIP3-4 short and RIP3-12 long respectively. Physiochemical and mechanical characterization and their potential application as drug depots are also studied. The characterization tests used for this study include biochemical assays, ultrasound, electron microscopy imaging, flow cytometry, dynamic light scattering measurements, and cell assays. The following are the research objectives of the thesis project.

1.2. Research Objectives

The research objectives of this thesis will be achieved by the following aims:

Aim1: Study of RIP1/RIP3 peptides aggregation, physiochemical and mechanical characterization.

Aim2: Study the mechanism of cellular uptake, investigate the potential of the aggregates as drug delivery depots.

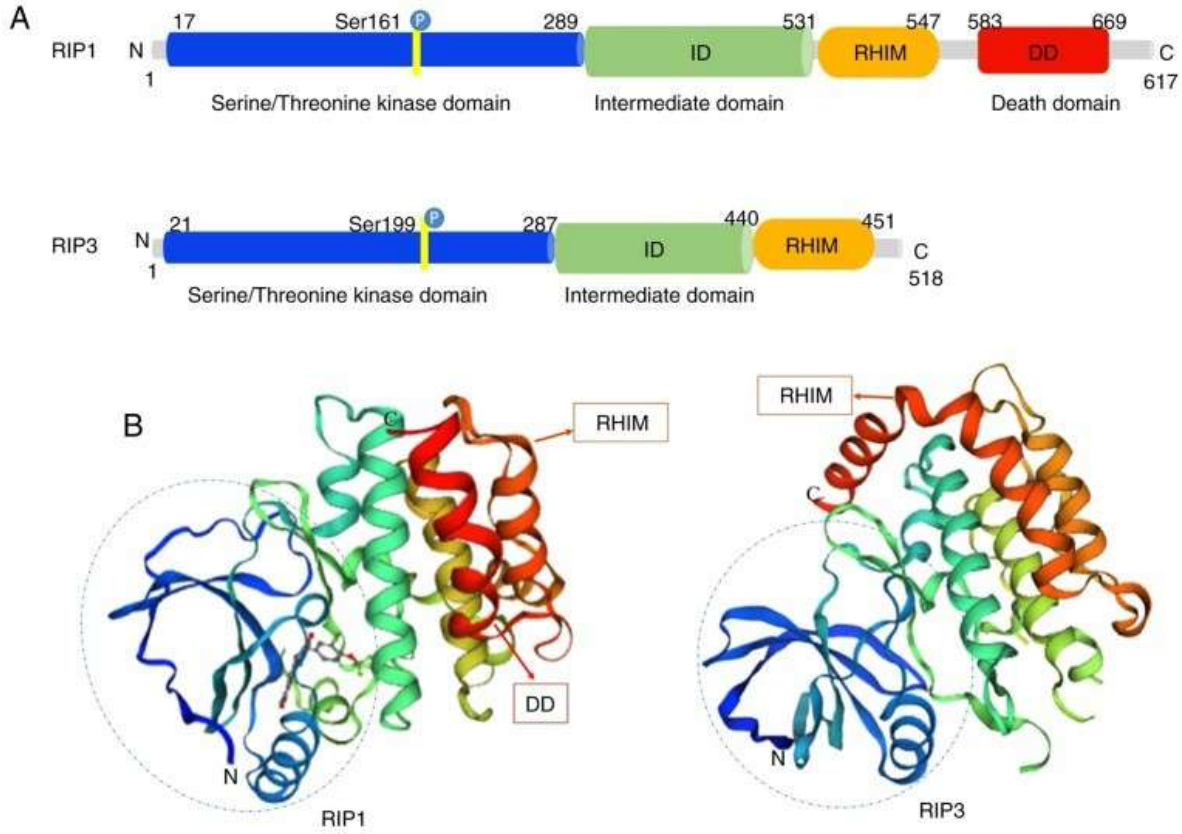

Figure 1.1 Structural diagrams of RIP1 and RIP3 (A). Schematic of functional domains of RIP1 and RIP3 proteins (B). Protein tertiary structure of RIP1 and RIP3 [4].

1.3. Thesis Organization

This thesis is organized into five chapters. Chapter 2 is a general background of RIP1/3 proteins and aggregation. The intention of the background is to provide the context for the motivation and goals of this work and to include an outline of the specific objectives of this work. Chapter 3 covers the approaches used to study the RIP1/3 peptide aggregates. Chapter 4 is the results from the thesis study. Finally, chapter 5 includes general conclusions and a summary of the contributions of this work. The thesis study could aid in novel insights on RIP1/RIP3

aggregation, which could be useful in understanding their role in multiple cellular functions and diseases.

1.4. References

[1] Soto, C., & Sandra, P. (2018). Protein Misfolding, Aggregation, and Conformational Strains in Neurodegenerative Diseases. *Nature Neuroscience*, *21*, 1332-1340.

[2] Hafner-Bratkovic, I. (2017). Prions, Prionoid Complexes and Amyloids: the bad, the good and something in between. *Swiss Medical Weekly,147*.

[3] Meylan, E., & Tschopp, J. (2005). The RIP kinases: crucial integrators of cellular stress. *Trends Biochem Sci, 30*, 151-159.

[4] Liu, Y., Liu, T., Lei, T., Zhang, D., Du, S., Girani, L., Qi, D., Lin, C., Tong, R., & Wang, Y. (2019). RIP1/RIP3-Regulated Necroptosis as a Target for Multifaceted Disease Therapy (Review). *International Journal of Molecular Medicine*, *44*, 771-786.

[5] Wu, X., Hu, H., Dong, X., Zhang, J., Wang, J., Schwieters, C.D., Liu, J., Wu, G., Li, B., Lin, J., Wang, H., & Lu, J. (2012). The Amyloid Structure of Mouse RIPK3 (Receptor Interacting Protein kinase 3) in Cell Necroptosis. *Nature News*, *12*.

[6] Li, J., McQuade, T., Siemer, A.B., Napetschnig, J., Moriwaki, K., Hsiao, Y., Damko, E., Moquin, D., Wals, T., McDermott, A., Chan, F., & Wu, H. (2012). The RIP1/RIP3 Necrosome Forms a Functional Amyloid Signaling Complex Required for Programmed Necrosis. *Cell, 150*(2), 339-350.

[7] Mompean, M., Li, W., Li, J., Laage, S., Siemer, A.B., Bozkurt, G., Wu, H., & McDermott, A.E. (2018). The Structure of the Necrosome RIPK1-RIPK3 Core, a Human Hetero-Amyloid Signaling Complex. *Cell*, *173*(5), 1244-1253.e10.

Chapter 2 : Background

2.1. Protein Aggregation

Understanding the processes of protein folding and misfolding have been a major research area from the last several decades in biology, chemistry, and physics [1]. Protein folding and misfolding is a complex biological phenomenon, and continues to motivate researchers to work both experimentally, and theoretically to fully understand the process. Misfolding protein may result in various manifestation of diseases. Proteins play a very crucial role in essential characteristics of living systems. Proteins are the most important classes of molecules which are involved in promoting and regulating essentially all the reactions which take place in living systems. Protein is a chain of amino acids bound to one another by peptide bonds like a string of beads. These strings get twisted and folded into a final protein shape. Most amino acids have a central carbon atom bonded to one amino group and one carboxylic acid (carboxyl) group [2]. The amino acids are held together by peptide bonds. There are four levels of protein structures: Primary, Secondary, Tertiary, Quaternary [3]. The secondary structure where the folding start to appear, the sequence of amino acids can fold in different ways. The most common ways are the alpha helix and the beta pleated sheet and play a major role in protein aggregation when folded incorrectly. Different proteins have different order of amino acids in the polymeric sequence. Usually, after the synthesis of the proteins, most of them must be converted into tightly folded compact structures in order to carry out function in proper way. Many of these structures are

complex, due to the fact that folding is usually very efficient [5,6].

The “Nomenclature Committee of the International Society of Amyloidosis” gave a universal definition for amyloid fibrils as ‘an insoluble protein fibril that is deposited, mainly, in the extracellular spaces of organs and tissues as a result of a sequence of changes in protein folding those results in a condition known as amyloidosis’ [7]. The main causes of protein aggregation include genetic mutations which is a result of substitution, addition, or deletion of amino acids due to radiation, chemicals, and infectious agents. Change in environmental conditions of the cell can lead to dysfunction of protein Quality Control (PQC) system or the mitochondria and the creation of unwanted interactions with folding proteins; the post-translational accidental changes the polypeptide after RNA-translation into amino acids [8]. The aggregation of proteins is mostly related with the perturbation of cellular function, ageing and various human disorders [9]. Ageing, mutation, and environmental stress etc. drive the proteins to deviate from their normal folding pathway that leads to the formation of protein aggregates/amyloids [10]. Apart from a pathological role, protein aggregation has also been found to be useful in memory, storage, scaffolding, and necrosis among others. Protein aggregation has been reported in various signaling processes. Receptor interacting protein kinases 1, 3, and RIP1/RIP3 complex in nephroptosis are some examples of protein aggregation in normal physiological function [11].

2.2. Receptor Interacting Protein (RIP) Kinases

Receptor interacting protein RIP kinases include seven members, all have a kinase domain (KD), and are important regulators of cell death and survival [12]. Among them, RIP1 and RIP3 are critical signaling molecules in necroptosis and is regulated by the caspase pathway [11]. It has been shown that the amyloid complex formed by receptor interacting protein (RIP) kinases1 and 3 is critical for the necroptosis process. Structurally, RIP1 and RIP3 share nearly half of their

amino acid sequences and have similar features [13]. RIP1 and RIP3 interaction is mediated by the RHIM region of the proteins.

2.2.1. RIP1 Kinase

RIP1 acts as a main switch of cell destiny regulation. Depending on the cellular context, RIP1 controls whether the pleiotropic cytokine tumor necrosis factor alpha (TNF-alpha) induces NF-kB activation, apoptosis, or programmed necrosis [14]. RIP1 receptor-interacting serine/threonine kinase1 was firstly identified in 1995 [15]. The RIP 1 protein has 671 amino acids. It contains a N-terminal serine/threonine kinase domain (KD) 1 to 289 amino acids, about 300 amino acids, and intermediate domain (ID) 290 to 582 amino acids, about 300 amino acids, and death domain (DD) 583 to 671, about 90 amino acids. The intermediate domain contains RIP homotypic interaction motif (RHIM) 531 to 547 amino acids, about 15 amino acids [13]. RIP1 perform as adaptors protein in response to the activated signal of death receptors (DRs). The kinase domain has varied function in cell survival, and it is important for necroptosis induction. The intermediate domain has the (RHIM) that enables the protein to combine with RIP3. In the death domain it binds to the death receptor of TNFR1, Fas, and TNF -related apoptosis inducting ligand (TRAIL) [16]. The assembly of the pro-necrotic RIP1–RIP3 complex is mediated through the “RIP homotypic interaction motif” (RHIM) [14].

2.2.2. RIP3 Kinase

RIP3 receptor-interacting serine/threonine kinase 3 was discovered in 1997 [17].

The RIP3 protein has 518 amino acids. It contains a N-terminal serine/threonine kinase domain (KD) 1 to 287 amino acids, about 300 amino acids, and intermediate domain (ID) 286 to 451 amino acids, about 165 amino acids, and unique C-terminal without death domain (DD) 452 to 518, about 70 amino acids. The intermediate domain contains RIP homotypic interaction motif

(RHIM) 440 to 451, about 10 amino acids [13]. RIP homotypic interaction motif (RHIM) is also present in the intermediate domain of RIP1, mediates RIP3 interaction with RIP1 and necrosis [18]. The death domain (DD) like in RIP1 can activate the transcription factor NFkB and when it expressed in the cells it can induce apoptosis [19].

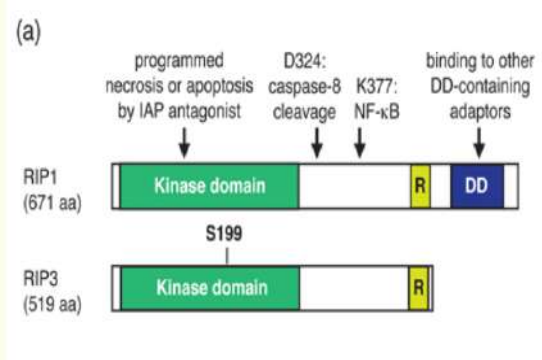

Figure 2.1 Diagram of RIP1, RIP3 Proteins (a) Schematic diagram of RIP1, RIP3 proteins containing RHIMS (R), Death Domain (DD). The arrows indicate the amino residues and domains important for RIP1 function. S199 is a reported necrosis-specific phosphorylation target site on RIP3 [14, 20].

2.2.3. RIP1 RIP3 Regulated Necroptosis

Necroptosis is mediated by a signaling complex called necrosome, containing receptor-interacting protein RIP1, RIP3, and mixed-lineage kinase domain-like (MLKL). It is known that RIP1 and RIP3 form heterodimeric filamentous scaffold in necrosomes through their RIP homotypic interaction motif (RHIM) domain-mediated oligomerization, but the signaling events based on this scaffold has not been fully addressed [21]. Necroptosis is another path of regulated cell death, usually apoptosis and necrosis are the main mechanisms of cell death. Necroptosis is a programmed form of necrosis. Many studies described apoptosis as the only form of programmed cell death (PCD), and necrosis as the accidental death path [22]. Necroptosis is regulated necrotic cell death mode in a caspase independent and is mainly mediated by RIP1, RIP3, and mixed lineage kinase domain-like (MLKL). Necroptosis can cause strong adaptive immune responses to defend against tumor development, so it has role for fighting cancer [23].

RIP1 and RIP3 are important effectors in the cell death regulating cellular survival, apoptosis, and necroptosis. RIP1 and RIP3 necrosome forms amyloid signaling complex required for regulated necrosis [24]. The present nomenclature states necroptosis as cell death mediated by signal transduction from receptor-interacting serine/threonine kinase RIP1 to RIP3, and it is called RIP1/RIP3. RIP3 dependent cell death is mostly used for necroptosis, so RIP3 is essential for necroptosis, while RIP1 is not dependably involved in the signal transduction. Particularly, deletion of RIP1 even promotes RIP3 mediated necroptosis in certain conditions [13].

Tumor Necrosis Factor alpha (TNF-α) is an inflammatory cytokine produce from macrophages/monocytes and it is responsible for different range of signaling with cells leading to apoptosis and necrosis [25]. TNF-α- induced RIP1/RIP3 interaction engages RIP3 recruitment, leading to RIP1/RIP3 homo-oligomerization and RIP3 autophosphorylation [13]. The binding of TNF to tumor necrosis factor receptor (TNFR) leads to recruitment of multiple proteins including RIPK1, and the protein complexes I. Therefore, the RIPK1 induces the NFkB pathway which transactivates cytoprotective genes and supports cell survival. Destabilization of complex I results in the formation of complex IIa that contains caspase-8. When cIAPs are blocked, and RIP1 deubiquitylated by CYLD, complex IIb is formed. This complex contains RIP1, RIP3, and caspase-8. Both complex IIa and complex IIb can initiate apoptosis. When caspase-8 is inhibited, RIP1 can bind to RIP3 to form RIP1/3 complex by intramolecular auto- and trans-phosphorylation. Then RIP3 recruits and phosphorylates MLKL to form complex IIc referred as necrosome. The phosphorylated MLKL then translocate from the cytosol to the plasma. Then oligomerization of MLKL result in necrosis (Figure 2.2) [13].

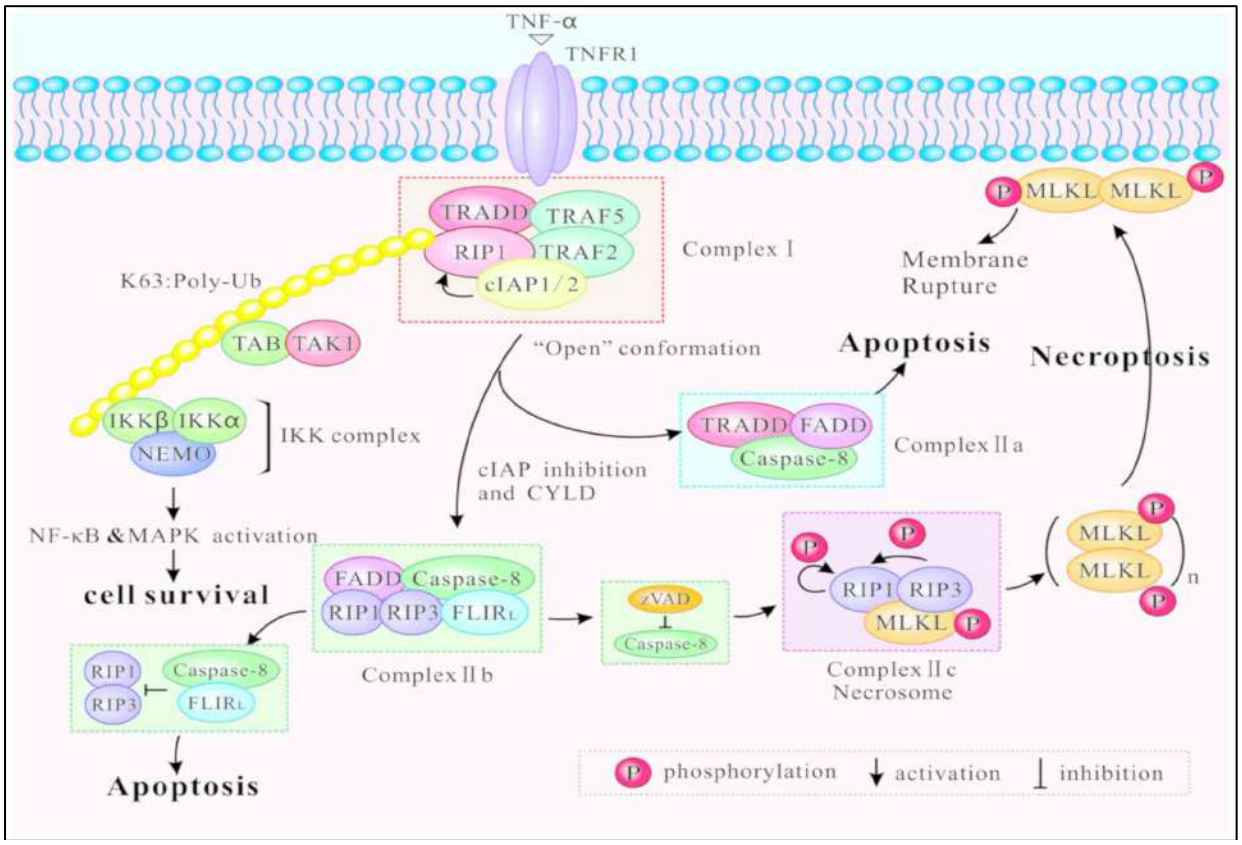

Figure 2.2 Mechanisms of RIP1/RIP3-regulated necroptosis [13]

2.3. RIP1, RIP3 Peptides and Proteins Aggregation

2.3.1. RIP1, RIP3 Protein Aggregation

RIP1 protein has 671 amino acids, and RIP3 has 518 amino acids. RIP1 has a N- terminal kinase domain (KD), an intermediate domain where RIP homotypic interaction motif (RHIM), and a C-terminal death domain (DD). RIP3 has a N-terminal kinase domain (KD), an intermediate domain where RIP homotypic interaction motif (RHIM). (RHIM) of RIP1 can binds to (RHIM) in RIP3 to form amyloid like structure and subsequently activate necroptosis [26]. (Figure 2.3) shows the structure of RIP1 and RIP3 protein.

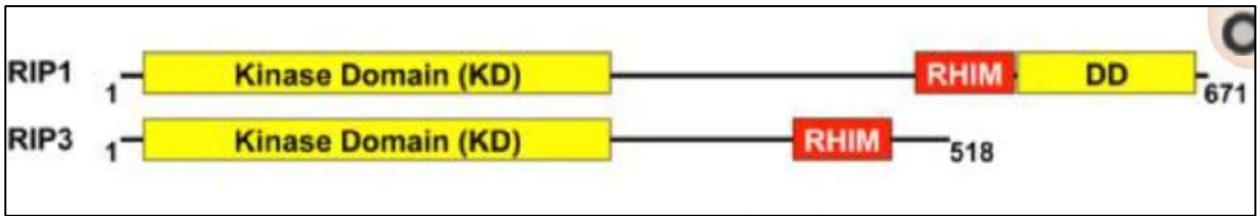

Figure 2.3 Domain organization of human RIP1 and RIP3 [24].

Studies showed that RIP1 by itself and RIP3 by itself cannot form an amyloid structure, but it can form amyloid structure through the RIP homotypic interaction motif (RHIM), and the amyloid is a functional signaling complex that leads to necrosis [24]. Studies still does not have a clear picture about the mechanism of RIP1 and RIP3 amyloid aggregates kinase activation, but it can be the beginning for further research about the amyloid structure.

2.3.2. RIP1, RIP3 Peptide Aggregation

The accurate boundaries of RHIMs that is responsible for the amyloid structure formation are still unclear, but the sequence conservation is centered around IQIG for RIP1, and VQVG for RIP3, (Figure 2.4) [24]. The residues IQIG and VQVG are conserved across different species are [14]. RHIMs of RIP1 (residues 496–583) and RIP3 (residues 388–518) (RIP1/3-RHIM) has shown to form amyloid like structure [27]. Beta sheet conformations predicted in RIP1 and RIP3 are shown in (figure 2.4). RIP1/3-RHIM might form large complexes. Further it has been reported that the region between the KD and the DD in RIP1 (residues 300–560) and the region C-terminal to the KD in RIP3 (residues 300-end) are unstructured random coils [28]. Based on the above findings, for this thesis study, small peptides sequences of RIP1 and RIP3 comprising of 4 amino acids sequences and 12 amino acids sequences in the RHIM region are chosen to check how RIP1 and RIP3 peptides aggregation characteristics and their potential role in necroptosis and in therapeutic applications. The sequences chosen for the study are: RIP1 peptides IQIG, and TIYNSTGIQIGA; RIP3 peptides VQVG and NIYNCSGVQVGD.

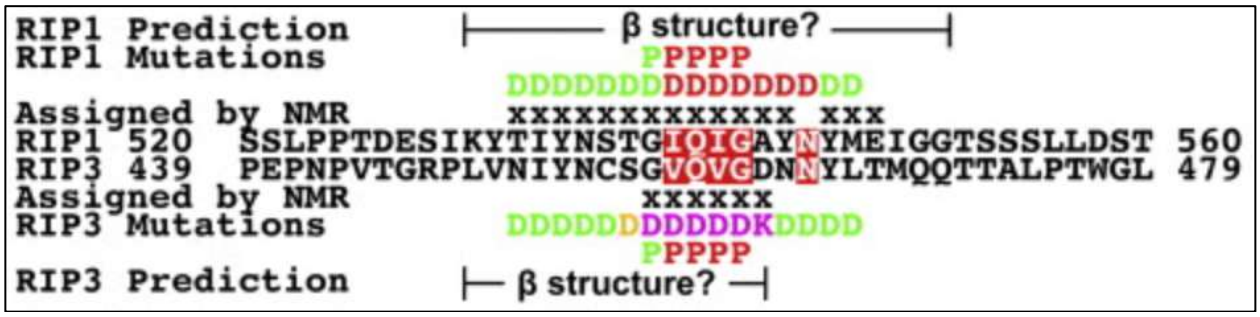

Figure 2.4 The peptide sequences of RIP1 and RIP3 around the core RHIM [24].

2.4. RIP1/3 Protein Aggregates in Therapeutic Applications

The use of RIP1/3 protein aggregates as therapeutic such as drug depots has not been explored. Protein aggregates have the added advantage compared to conventional nanocarriers due to inherent therapeutic properties, tunability, biodegradability, and biocompatibility. Hence, RIP1/RIP3 aggregates could be utilized as drug delivery vesicles. In addition, due to their inherent role in necroptosis, they could be tuned to induce necrosis, and could be utilized for multifunctional purpose. Further, recent studies suggest RIP1/3 necroptosis as a target for multi disease therapy including cancer [29]. This thesis work includes the study to understand cellular uptake mechanism of the RIP1/RIP3 peptide aggregates, and their potential as drug delivery depot. For the cell transport mechanism, endocytosis mediated uptake is assessed, and for the drug depot, cisplatin is used as model drug and the effect in cancer cells is studied.

2.5. References

[1] Stefani, M. (2008, December 10). Protein folding and misfolding on surfaces. *International Journal of Molecular Sciences, 9* (12), 2515-2542.

[2] Bischoff, R., & Schlüter, H. (2012, February 22). Amino acids: Chemistry, functionalityand selected non-enzymatic post-translational modifications. *Journal of Proteomics*, *75*(8),2275-2296.

[3] Moutevelis, E., & Woolfson, D. N. (2009, January 23). A periodic table of coiled-coil protein structures. *Journal of Molecular Biology, 385*(3), 726-732.

[4] Soto, C., & Sandra, P. (2018). Protein Misfolding, Aggregation, and Conformational Strains in Neurodegenerative Diseases. *Nature Neuroscience*, *21*, 1332-1340.

[5] Balchin, D., Hayer-Hartl, M., & Hartl, F. U. (2016). In vivo aspects of protein folding and quality control. *Science, 353*, 4354.

[6] Gruebele, M., Dave, K., & Sukenik, S. (2016). Globular protein folding in vitro and In vivo. *Annu. Rev. Biophys., 45*.

[7] Westermark, P. (2005). Aspects on human amyloid forms and their fibril polypeptides. *Febs Journal, 272* (23), 5942-5949.

[8] Scheibel, T., & Buchner, J. (2006). Protein aggregation as a cause for disease. *Handbook of experimental pharmacology,* 199-219.

[9] Alam, P., Siddiqi, K., Chturvedi, S. K., & Khan, R. H. (2017, May 15). Protein aggregation: From background to inhibition strategies. *International Journal of Biological Macromolecules, 103*, 208-219.

[10] Hipp, M.S., Park, S.H., & Hartl, F.U. (2014). Proteostasis impairment in protein-misfolding and aggregationdiseases. *Trends Cell Biol.,24*,506-514.

[11] Newton, K. (2015, February 4). RIPK1 and Ripk3: Critical regulators of inflammation and cell death. *Trends in Cell Biology, 25*(6), 347-353.

[12] Meylan, E., & Tschopp, J. (2005). The RIP kinases: crucial integrators of cellular stress. Trends Biochem Sci, 30, 151-159.

[13] Liu, Y., Liu, T., Lei, T., Zhang, D., Du, S., Girani, L., Qi, D., Lin, C., Tong, R., & Wang, Y. (2019). RIP1/RIP3-Regulated Necroptosis as a Target for Multifaceted DiseaseTherapy (Review). *International Journal of Molecular Medicine, 44*, 771-786.

[14] Moquin, D., & Chan, F.K. (2010). The molecular regulation of programmed necrotic cell injury. *Trends Biochem. Sci.,* 35,434-441.

[15] Stanger, B.z., Leder, P., Lee, T., Kim, E., & Seed, B. (1995, May 19). RIP: A novel protein containing a death domain that interacts with Fas/ APO-1 (CD95) in yeast and causes cell death. *Cell, 81*(4), 513-523.

[16] Wen, L., Zhuang, L., Luo, X., & Wei, P. (2003, October 3). TL1A-induced NF-KB activation and C-IAP2 production prevent DR3-mediated apoptosis in TF-1 cells. *Journal of Biological Chemistry*, *278*(40), 39251-39258.

[17] Sun, X., Lee, J., Navas, T., Baldwin, D. T., Stewart, T. A., & Dixit, V. M. (1999, June 11). RIP3, a novel apoptosis-inducing kinase. *Journal of Biological Chemistry*, *274*(24), 16871-16875.

[18] Moriwaki, K., & Chan, F. K.-M. (2013, August 1). RIP3: A molecular switch for necrosis and inflammation. *Genes & development, 27*(15), 1640-1649.

[19] Yu, P., Huang, B.C.B., Shen, M., Nolan, G.P., Payan, D.G., & Luo, Y. (1999, May 20). Identification of RIP3, a RIP-like kinase that activated apoptosis and NFkB. *Brief Communications, 9*(10), S1-S3.

[20] Degterev, A., Hitomi, J., Germscheid, M., Ch'en, I. L., Korkina, O., Teng, X., Abbott, D., Cuny, G. D., Yuan, C., Wagner, G., Hedrick, S. M., Gerber, S. A., Lugovskoy, A., & Yuan, J. (2008, May). Identification of RIP1 kinase as a specific cellular target of Necrostatins. *Nature chemical biology,4*(5), 313-321.

[21] Wu, X.-N., Yang, Z.-H., Wang, X.-K., Zhang, Y., Wan, H., Song, Y., Chen, X., Shao, J., & Han, J. (2014, November). Distinct roles of Rip1-Rip3 hetero- and Rip3-Rip3 homo-interaction in mediating necroptosis. *Cell death and differentiation,21*(11),1709-1720.

[22] Linkermann, A., & Green, D.R. (2014, January 30). Necroptosis. *New England Journal of Medicine,370*, 455-465.

[23] Gong, Y., Fan, Z., Luo, G., Yang, C., Huang, Q., Fan, K., Cheng, H., Jin, K., Ni, Q., Yu, X., & Liu, C. (2019, May 23). The role of Necroptosis in cancer biology and therapy. *Molecular Cancer,100*(18).

[24] Li, J., McQuade, T., Siemer, A.B., Napetschnig, J., Moriwaki, K., Hsiao, Y., Damko, E., Moquin, D., Wals, T., McDermott, A., Chan, F., & Wu, H. (2012). The RIP1/RIP3 Necrosome Forms a Functional Amyloid Signaling Complex Required for Programmed Necrosis. *Cell,150*(2), 339-350.

[25] Idriss, H. T., & Naismith, J.H. N. (2000, August 1). TNF alpha and the TNF receptor superfamily: Structure-function relationship(s). *Microscopy research and technique, 50*(30, 184-195.

[26] Zhe-Wei, S., Li-Sha, G., & Yue-Chun, L. (1AD, January 1). The role of necroptosis in cardiovascular disease. *Frontiers.*

[27] Sun, L., Wang, H., Wang, Z., He, S., Chen, S., Liao, D., Wang, L., Yan, J., Liu, W., Lei, X., & Wang, X. (2012, January 19). Mixed lineage kinase domain-like protein mediates necrosis signaling downstream of rip3 kinase. *Cell, 148*(1-2), 213-227.

[28] Rost, B., Yachdav, G., & Liu, J. (2004, July 1). The predictprotein server. *Nucleic acids research*, *32*, W321-W326.

[29] Lin, Y., Devin, A., Rodriguez, Y., & Liu, Z. G. (1999, October 1). Cleavage of the death domain kinase rip by caspase-8 prompts TNF-induced apoptosis. *Genes & development*, *13*(19), 2514-2526.

Chapter 3: Materials and Methods

3.1. Materials

Receptor interacting protein RIP 1 and RIP 3 peptides were custom synthesized from Genscript. The other materials and reagents were bought from either Thermo Fisher Scientific or Sigma Aldrich (St. Louis, MO).

3.2. Physicochemical Characterization

Peptide aggregation was performed using two peptide sequences. The sequences are IQIG, TIYNSTGIQIGA, VQVG, NIYNCSGVQVGD of RIP1 and RIP3 respectively. To form the aggregation, first peptides stock solutions in DMSO at 10 mM concentration was prepared. From the stock solutions, 20μM, 100μM, or 1 mM concentrations of peptides where prepared by dissolving with buffers 20 mM MOPS, pH 7 or 20 mM Ammonium Acetate, pH 7 or 100 mM Ammonium Acetate, pH7. All buffers were filtered prior to use through 0.22 μm nylon, sterile filter. The aggregation was performed at around 37 degrees Celsius in a thermomixer in the lab. Peptide aggregates were also performed with FITC-labelled peptides for detection in cellular assays. The peptide aggregation process was then characterized by Thioflavin-T (ThT), Congo Red, Dynamic Light Scattering (DLS), Turbidity, and Transmission electron microscopy (TEM) measurements.

3.2.1. ThT Fluorescence

1 mM ThT stock was prepared in water. The solution was then dissolved in 20 mM Trizma hydrochloride solution (Tris) pH 8 to obtain 50 μM ThT. 5 μl of the peptide aggregate sample

was mixed with 100 µl of the 50 µM ThT, and the aggregation kinetics was measured at 0 hour, 1 day, and 7 days. The excitation wavelength is 440 nm, and the emission wavelength is 482 nm. The ThT fluorescence was measured in the laboratory at these wavelengths using the SpectraMax M3 Spectrophotometer from Molecular Devices. The experiments were repeated four times.

3.2.2. Congo Red

Congo red stock solution was prepared by dissolving 1 mg of congo red in 4.5 ml of DI water and 500 µl of ethanol mixture. For the characterization, 15 µl of the congo red solution was mixed with 85 µl of 50 µl peptide aggregate, and the absorbance spectra was obtained from 400-700 nm using the SpectraMax M3 spectrophotometer in the lab. The aggregation kinetics was measured at 0 hour, 1 day, and 7 days. The experiments were repeated four times.

3.2.3. Dynamic Light Scattering (DLS)

To measure the aggregate size, dynamic light scattering measurements were performed using a Malvern Zetasizer instrument in the laboratory. For the size measurements, 5 µl of the peptide was mixed with 50 µl buffer. The zeta size was measured at 0 hour, 1 day, and 7 days aggregation time points. Measurements were carried out for four different experiments.

3.2.4. Turbidity

For the turbidity measurements at the first attempt. 5 µl of the peptide aggregates was used and was diluted with 95 µl buffer. The measurements did not show significant change in absorbance compared to the buffer alone. Hence, as a second attempt 100 µl of the peptide aggregates was used to measure the turbidity. The measurements were performed at 400 nm, 600 nm wavelength. The turbidity measurements were measured at 0 hour, 1 day, and 7 days from the

start of the aggregation, using the SpectraMax M3 Spectrophotometer from Molecular Devices in the laboratory. Similar to other characterization studies, experiments were repeated four times.

3.2.5. Transmission Electron Microscopy (TEM)

To determine the morphology of the aggregate TEM imaging was performed. First, formvar carbon 200 mesh copper grids were plasma treated. Then 5 µl of the sample was spotted on the copper grid, and then stained with 2% phosphotungstic acid pH 7.4. 0 hour and 1 day aggregation samples were used for the imaging. Imaging was performed using a JEOL TEM microscope at 80 kV, at the electron microscopy facility at the University of Michigan Ann Arbor medical school.

3.3. Mechanical Characterization

3.3.1. Ultrasound

To test whether the peptide aggregates exhibit mechano sensitive properties, ultrasound mediated mechano sensitive measurement were performed. Ultrasound was performed using ultrasonicator 740 from Mettler Electronic Corp (intensity 2.2 W/cm^2, 1 cm^2 applicator) in the laboratory. The sonication was applied either for 5 minutes or 10 minutes. The effect of ultrasonication on the aggregates was measured by DLS, and TEM imaging, as well as on cell assays.

3.4. Microscopy and Flow Cytometer Characterization

3.4.1. Flow Cytometry

Flow cytometry was used to measure apoptosis/necrosis, endocytosis uptake, and ultrasound mediated peptide aggregates. Flow cytometry measurement were performed using Attune Nxt Flow in the laboratory.

3.5. Cellular Assay

3.5.1. Cell Toxicity (alamarBlue) Assay

To measure the cellular toxicity, alamarBlue assay was performed. MDA MB 231 cells were obtained from ATCC (American Type Culture Collection) and cultured in DMEM, 10% fetal bovine serum, and 1% antibiotic-antimycotic according to the protocol. For the toxicity assay, cells were cultured in a 96 wells plate at a density of 10,000 cells/well. Then after 24 hours, cells were treated with 100 μM of RIP 1, RIP 3 peptide aggregates and subsequently incubated for additional 48 hours and alamarBlue assay was performed according to the manufactures protocol. The cell toxicity was assessed by the metabolic activity of the cells at 570/590 nm, excitation/emission of oxidation-reduction (REDOX) indicator. Experiments were repeated four times.

3.5.2. Cellular Uptake Experiment

The cells were cultured in 24 wells plate at a density of 100,000 cells/500 μl/well. Then after 48 hours the inhibitors were added to the cells. The inhibitors used were 5 μg/ ml of Chlorpromazine Hydrochloride (CPZ), 80 μM of Dynasore the Dynamin inhibitor, and 25 μg/ml of Cytochalasin D. The cells were incubated for 90 minutes after inhibitor treatment, and subsequently treated with 100 μM peptide aggregates for 30 minutes. Cellular uptake of the aggregates with and without the inhibitor was assessed by Attune Nxt Flow Cytometer in the laboratory. The experiments were repeated three times.

3.5.3. Apoptosis Necrosis Assay

The cells were cultured in 24 wells plate at a density of 100,000 cells/ 500 μl/well. Then after 24 hours, 100 μM RIP 1, RIP 3 peptides aggregates were added to the cells, and then incubated for additional 48 hours. Then apoptosis and necrosis were assessed by PI/Annexin V staining using

an apoptosis/necrosis kit from Biotium. The measurement was performed by the Invitrogen Attune Nxt Flow Cytometer from Thermo Fisher Scientific in the laboratory, and the experiments were repeated three times.

3.6. Statistical Analysis

All experiments for the thesis project were repeated at least three or more times. The data is represented as mean ± standard error (S.E.). Student T-test was used to determine the statistical significance, and data with significance is represented as * $p < 0.05$.

Chapter 4 : Results

4.1. Peptide Aggregation Characterization by Thioflavin T Fluorescence ThT

Two concentrations 20 μM, 100 μM of RIP1 and RIP3 short and long sequence were studied with two buffers 20 mM MOPS (3-(N-morpholino) propanesulfonic acid) PH7, and ammonium acetate (NH4OAC) with two different concentrations 20 mM, 100 mM (Table 4.1). Thioflavin T fluorescence measurements were performed using a SpectraMax M3 Spectrophotometer plate reader from Molecular Devices at the excitation wavelength of 440nm and emission wavelength of 482 nm.

Table 4.1. Shows the peptide concentration, buffer, and peptide sequence.

Peptide concentration	Buffer	Peptide sequence
20 μM, 100 μM	20 mM NH4OAC, pH 7	4 Amino Acids of RIP1 and RIP3: IQIG, VQVG. 12 Amino Acids of RIP 1 and RIP3: TIYNSTGIQIGA, NIYNCSGVQVGD
20 μM, 100 μM, 1 mM	100 mM NH4OAC, pH 7	4 Amino Acids of RIP1 and RIP3: IQIG, VQVG. 12 Amino Acids of RIP 1 and RIP3: TIYNSTGIQIGA, NIYNCSGVQVGD
20 μM, 100 μM	MOPS buffer, pH 7	4 Amino Acids of RIP1 and RIP3: IQIG, VQVG. 12 Amino Acids of RIP 1 and RIP3: TIYNSTGIQIGA, NIYNCSGVQVGD

As a first step, 20 µM RIP1 or RIP3 or RIP1/3 short sequence peptides, RIP1-4 (IQIG), RIP3-4 (VQVG), RIP1/RIP3 (10 µM each) were aggregated with all three buffer conditions, and peptide aggregation kinetics was measured at 0 day, 1 day, and 7 days. The aggregates did not exhibit aggregation in any of the days. Representative ThT data for 1 day aggregation is shown in (Figure 4.1). From (Figure 4.1) it can be seen no significant aggregation of the peptides was obtained at 20 µM concentrations in all three buffer conditions at 1 day. Next concentration was increased to 100 µM, and the ThT measurements were repeated. Again, the ThT measurement showed no significant peptide aggregation that compared the short sequence. Representative aggregation data at 1 day is shown in (Figure 4.2). So, 20 µM, and 100 µM short peptide sequence were aggregated in all 3 buffer conditions and ThT measurements were performed. No significant aggregation was observed in, and the short peptides were aggregated, and measurements were performed at 0 day, 1 day, and 7 days.

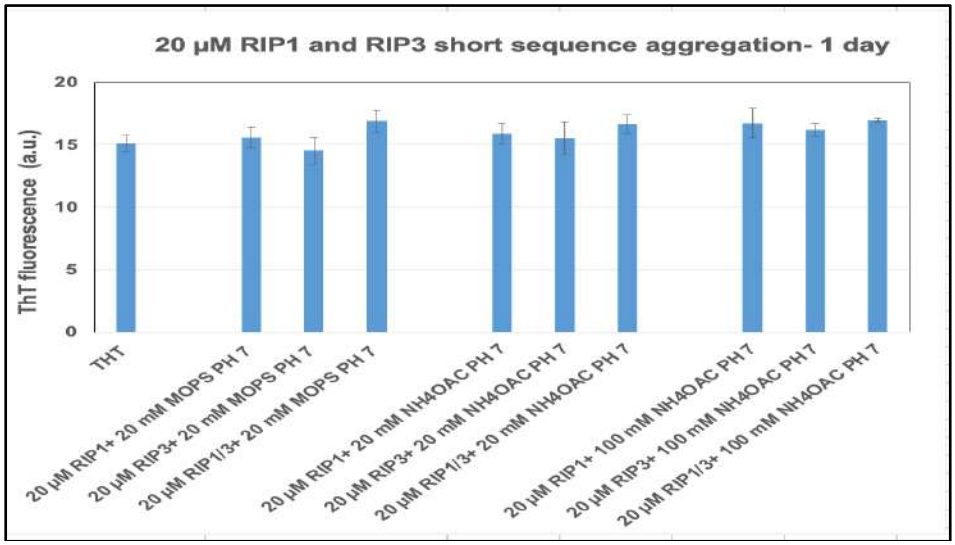

Figure 4.1 ThT Fluorescence of short sequence 20 µM RIP1-3, RIP3-4 with 20 mM MOPS PH7 buffer, 20 mM ammonium acetate PH7 buffer, 100 mM ammonium acetate PH7 buffer during 1 day of starting the peptide aggregation.

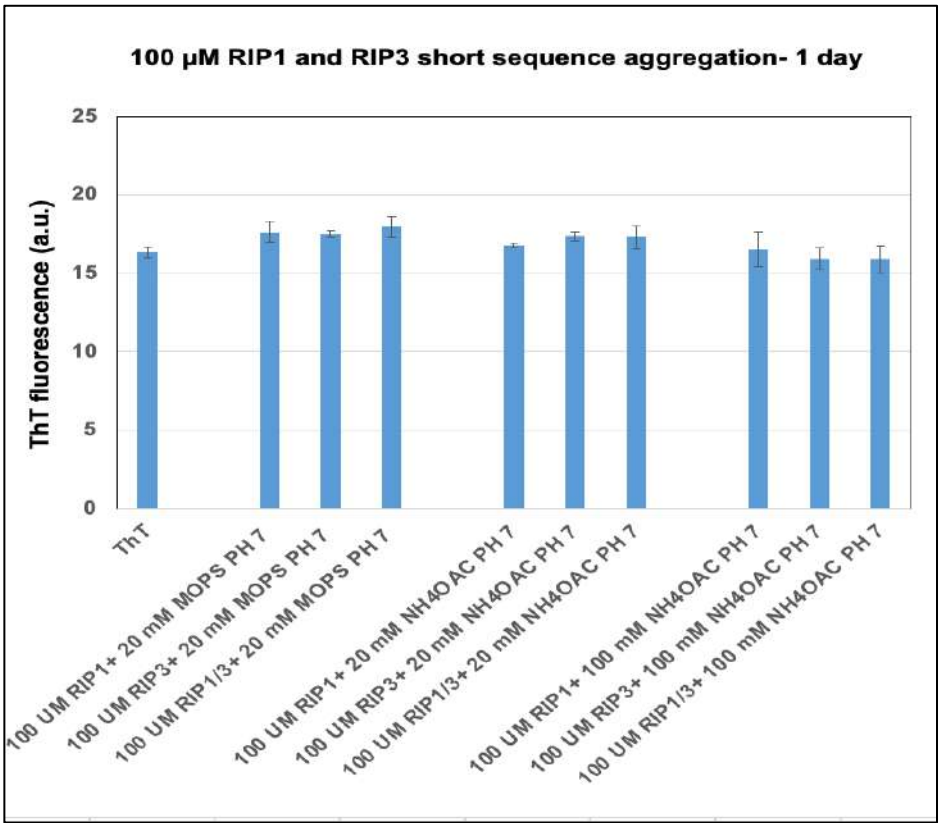

Figure 4.2 ThT Fluorescence of short sequence 100 µM RIP1-3, RIP3-4 with 20 mM MOPS PH7 buffer, 20 mM ammonium acetate PH7 buffer, 100 mM ammonium acetate PH7 buffer during 1 day of starting the peptide aggregation.

Then the long sequence with 12 amino acids of RIP1-12 (TIYNSTGIQIGA), RIP 3-12 (NIYNCSGVQVGD) and RIP1-12/RIP3-12 of 20 µM, and 100 µM was used. The aggregation in all 3 buffer conditions was studied. Among the conditions tested only 100 µM peptide in 100 mM NH4OAC buffer conditions showed aggregation with ThT as shown in (Figure 4.3).

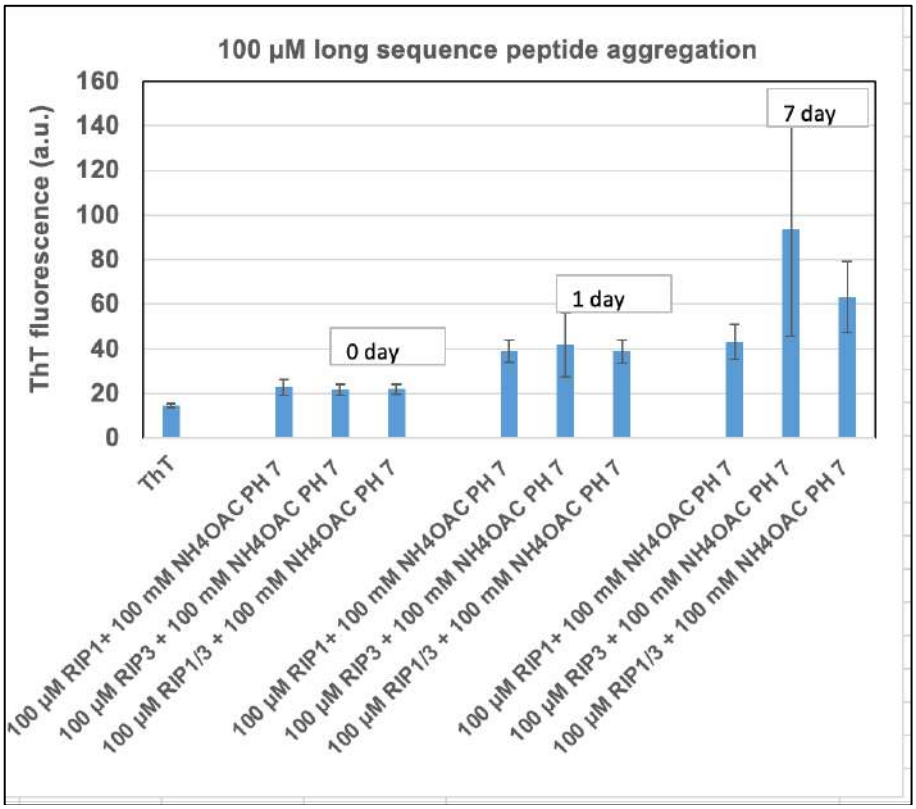

Figure 4.3 ThT Fluorescence of long sequence 100 µM RIP1-3, RIP3-4 with 100mM ammonium acetate PH7 buffer during 1 day of starting the peptide aggregation.

From the results, next 1mM concentration with 100 mM ammonium acetate PH7 buffer for the long sequence peptide aggregation was used, and also compared with the short sequence RIP1-4 (IQIG), RIP3-4 (VQVG), RIP1-4/RIP3-4 with the same conditions. The ThT data showed more significant peptide aggregation of the long sequence with 3 different time: 0 day (Figure 4.4), 1 day (Figure 4.5), 7 days (Figure 4.6). The short sequence showed no significant aggregation in 1mM peptide concentration as well. Based on ThT studies, the next study was concentrated on 1mM long sequence peptide aggregates.

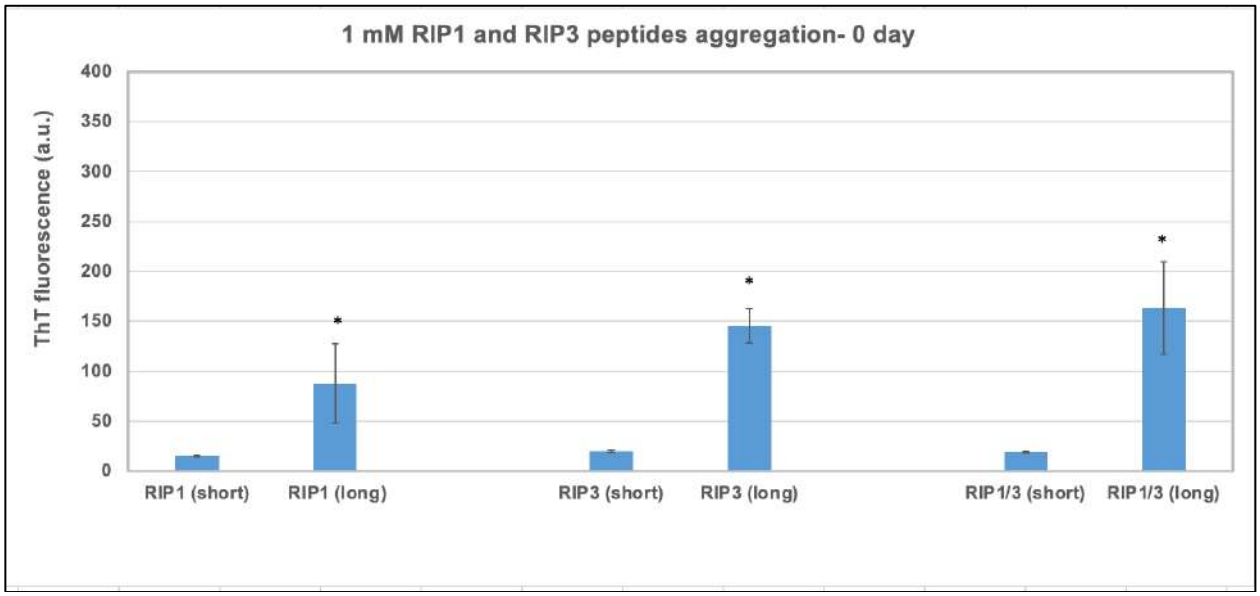

Figure 4.4 ThT Fluorescence of short and long sequence 1mM RIP1,RIP3 with 100 mM ammonium acetate PH7 buffer during 0 day of starting the peptide aggregation.

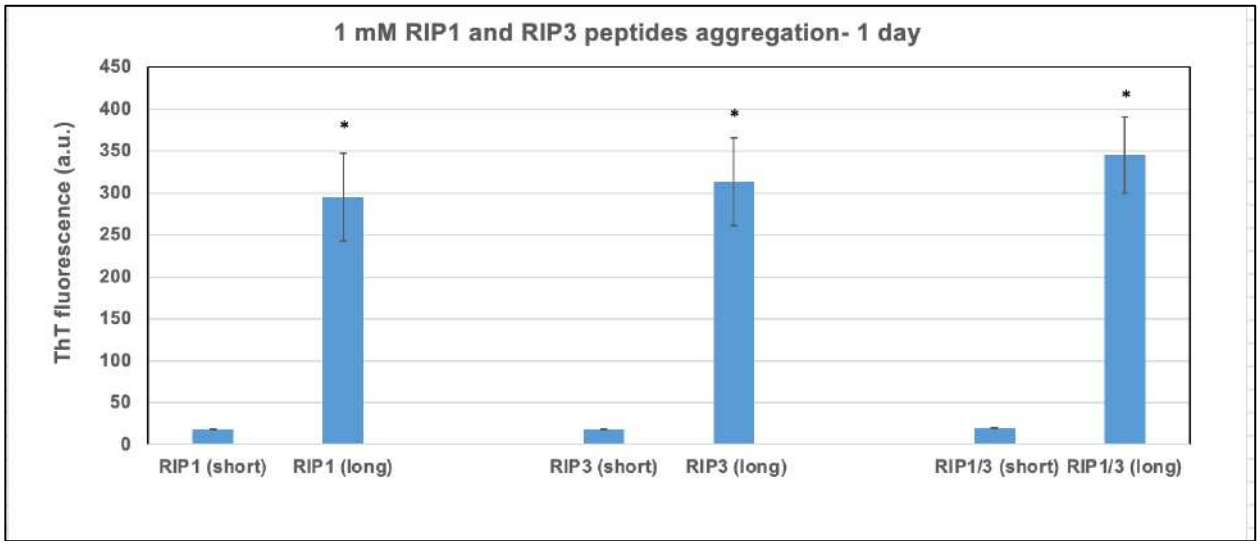

Figure 4.5 ThT Fluorescence of short and long sequence 100 mMRIP1, RIP3 with 100 mM ammonium acetate PH7 buffer during 1 day of starting the peptide aggregation.

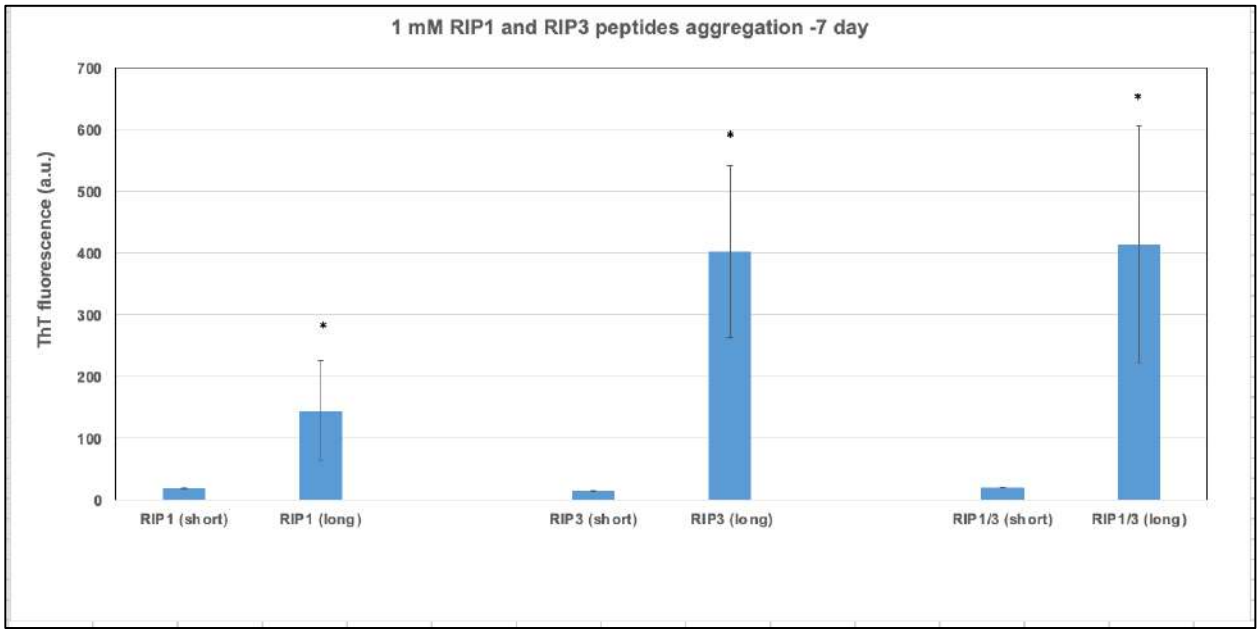

Figure 4.6 ThT Fluorescence of short and long sequence 100 mM RIP1, RIP3 with 100 mM ammonium acetate PH7 buffer during 7 days of starting the peptide aggregation.

4.2. Peptide Aggregation Characterization by Dynamic Light Scattering DLS

DLS measurements were performed using a Malvern Zetazsizer to predict the size of the peptide aggregation. DLS measurement of 1 mM of the long sequence peptide RIP1-12 (TIYNSTGIQIGA), RIP3-12 (NIYNCSGVQVGD), and RIP1-12/RIP3-12 was performed. The measurements were done at three different times 0 day, 1 day, and 7 days. The DLS data of the size measurements showed an increase in peptide size aggregation within time especially after 1 day of the aggregation. Representative images are shown in (Figure 4.7). The average size data is tabulated in (Table 4.2).

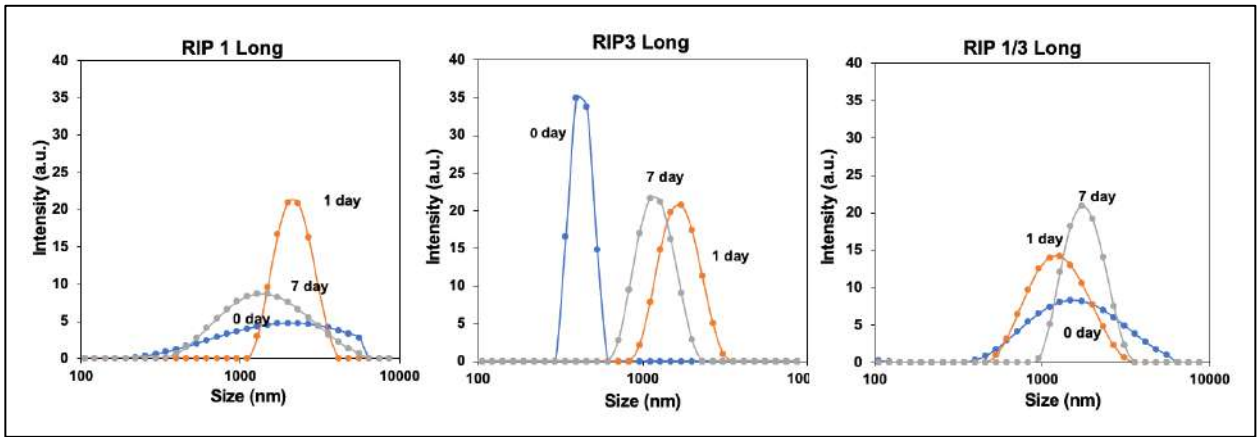

Figure 4.7 DLS measurements of 1mM peptide aggregation.

Table 4.2. DLS size data

1 mM Peptide Aggregates	0 Hour Zavg (nm)	1 Day Zavg (nm)	7 Day Zavg (nm)
RIP1	1029.275± 314.39	1331.875± 524.85	1168.1±103.05
RIP3	1633.5± 423.65	1681± 434.37	958± 260.04
RIP 1/3	1338 ± 658.31	2311.67 ± 96.18	1808 ± 168.50

4.3. Peptide Aggregation Congo Red

Congo red has been used in protein aggregation studies, due to its binding properties to amyloid fibrils and aggregates. Congo Red measurements were performed in 96-well plate on SpectraMax M3 Spectrophotometer plate reader from Molecular Devices. The absorption spectra were recorded from 400-700nm. 1 mM of the long sequence peptide RIP1-12 (TIYNSTGIQIGA), RIP3-12 (NIYNCSGVQVGD), and RIP1-12/RIP3-12 aggregates were used for the study. Also, 1 mM of the short sequence peptide aggregates RIP1-4 (IQIG), RIP3-4 (VQVG), and RIP1-4/RIP3-4 were prepared. The measurements were done at three different times 0 day, 1 day, and 7 days. Plots were generated for absorbance from 600-700 nm. All the measurement showed increasing of the absorbance of long peptide aggregates compared to short peptide aggregates in agreement with ThT study. (Figure 4.8).

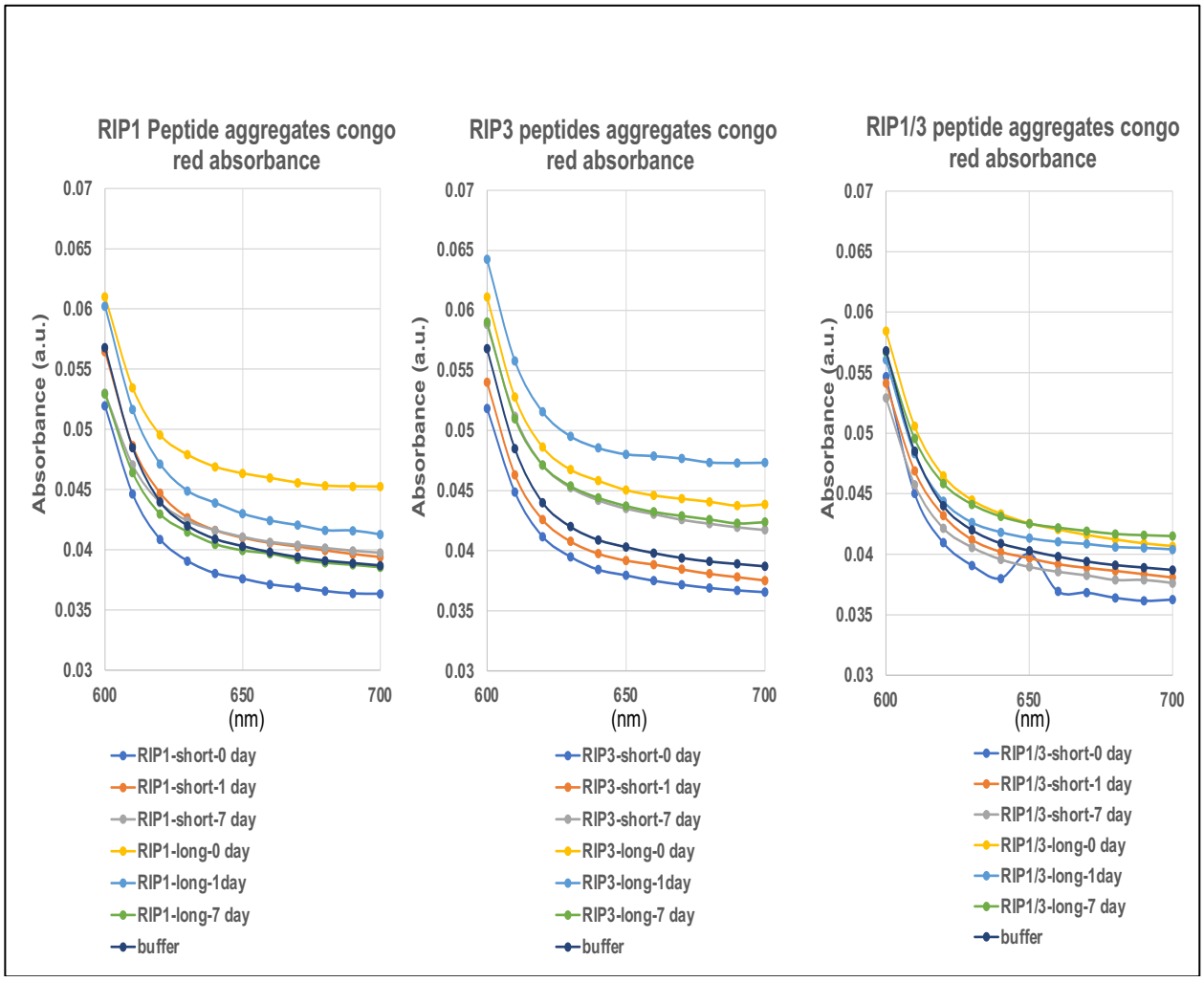

Figure 4.8 Congo Red measurements of short and long peptides aggregation. Measurements show an increase in absorbance for long peptide aggregates.

4.4. Turbidity

As another complementary characterization, turbidity measurements were performed using a SpectraMax M3 Spectrophotometer plate reader from Molecular Devices at 400 nm, 600 nm. 1 mM of the long sequence peptides aggregates RIP1-12 (TIYNSTGIQIGA), RIP3-12 (NIYNCSGVQVGD), and RIP1-12/RIP3-12 were prepared. Also, 1 mM of the short sequence peptide RIP1-4 (IQIG), RIP3-4 (VQVG), and RIP1-4/RIP3-4 aggregates were prepared. The measurements were done at three different times 0 day, 1 day, and 7 days. The results showed no

significant turbidity with the short peptides and significant turbidity with the long peptides for 1 day aggregates (Figure 4.9).

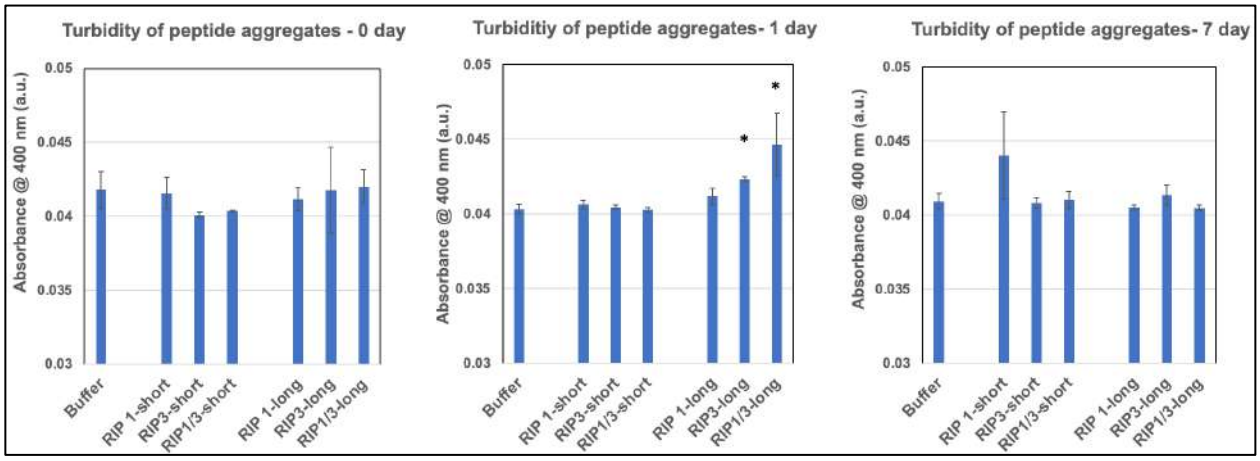

Figure 4.9 Turbidity measurements performed on short and long RIP1, RIP3 peptide aggregation samples at 400 nm at 0, 1, and 7 days. $p < 0.05$.

4.5. Morphology by TEM

To find the morphology of the samples at 0 day and 1 day aggregation, Transmission Electron Microscopy was performed using a JEOL TEM microscope at 80 kV, at the electron microscopy facility at the University of Michigan Ann Arbor medical school. 1 mM aggregates of the long sequence peptides RIP1-12 (TIYNSTGIQIGA), RIP3-12 (NIYNCSGVQVGD), and RIP1-12/RIP3-12 were prepared. The TEM images of peptides (Figure 4.10) were in agreement with the ThT, DLS measurements where the samples became more aggregate, and the size of fibrils increase after one day of peptides aggregation.

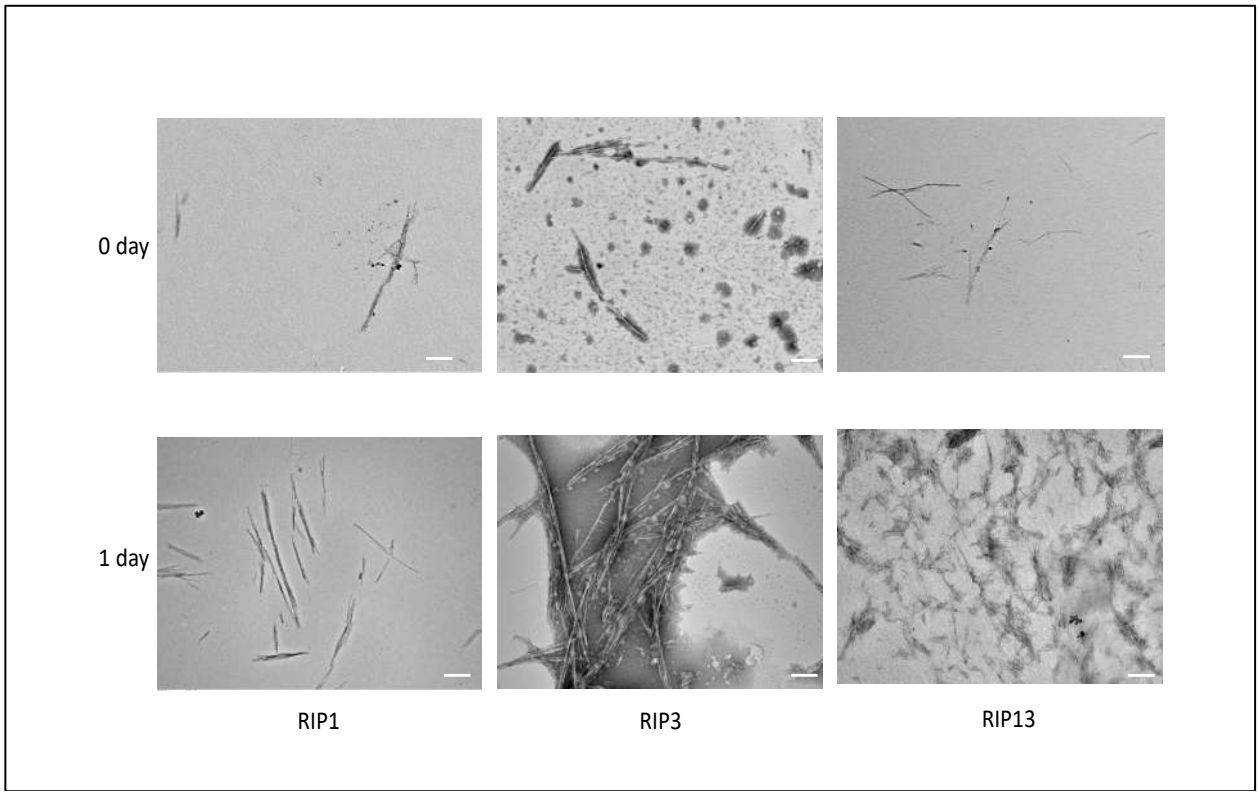

Figure 4.10 TEM images of RIP1, RIP3, RIP1/3 at 0 day, 1 day. Scale bar 200 nm

4.6. Mechanical Characterization

To test whether the peptide aggregates exhibit mechano sensitive properties, ultrasound mediated mechano sensitive measurement were performed. Ultrasound was performed using ultrasonicator 740 from Mettler Electronic Corp (intensity 2.2 W/cm^2, 1 cm^2 applicator) in the laboratory. The sonication was applied for 8 minutes. The effect of ultrasonication on the aggregates was observed by TEM imaging, 1 mM of the long sequence peptide aggregates was prepared, and after 1 day the peptide aggregates was subjected to ultrasound. The TEM images of the aggregates are shown in (Figures 4.11 ,4.12). From the images the aggregates show sensitivity to ultrasound.

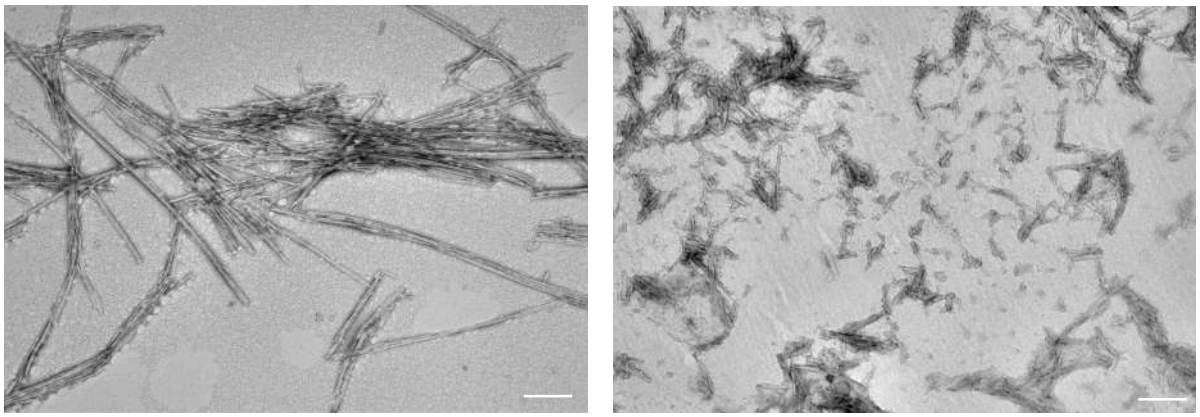

Figure 4.11 TEM images of RIP3, RIP3 ultrasound after 1 day aggregation. The ultrasound condition: 2.2 W/cm^2 intensity, 8 minutes.

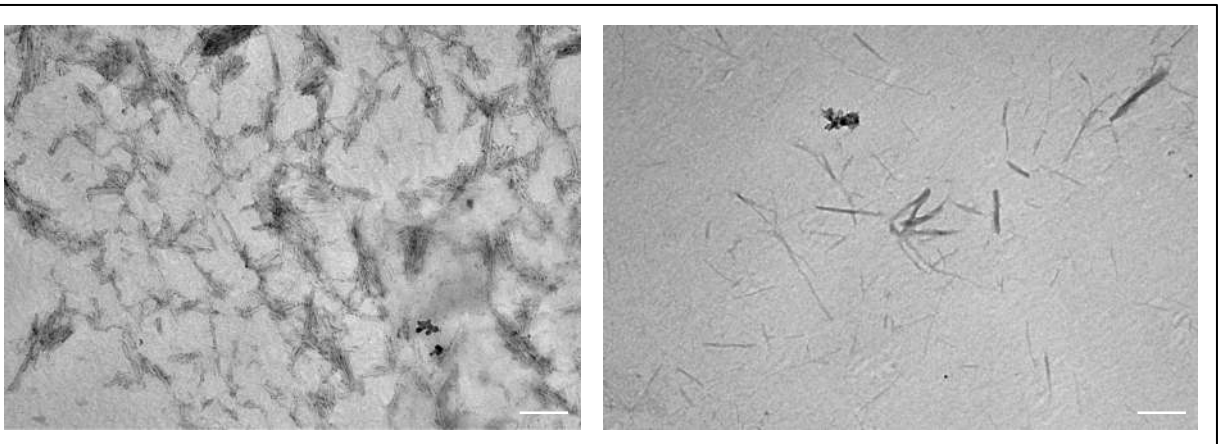

Figure 4.12 TEM images of RIP1/3, RIP1/3 ultrasound after 1 day aggregation. The ultrasound condition: 2.2 W/cm^2 intensity, 8 minutes.

4.7. Cellular Uptake with and Without Ultrasound

Cellular uptake with and without ultrasound was assessed by Attune Nxt Flow Cytometer from Thermo Fisher Scientific in the laboratory. Ultrasound was performed using ultrasonicator 740 from Mettler Electronic Corp (intensity was varied from 1.1- 2.2 W/cm^2, time was varied from 5-10 min) in the laboratory. The cells were cultured in 24 wells plate at a density of 100,000 cells/ 500 µl/well. Then after 48 hours the peptides aggregates were added to the cells. 1 mM of the long

sequence fluorescein labelled peptides aggregates RIP1-12 (TIYNSTGIQIGA), RIP3-12 (NIYNCSGVQVGD), and RIP1-12/RIP3-12 were prepared. After one day the labelled peptides added to the cells. Two different cell culture conditions were used for the ultrasound. Cells were either subjected to ultrasound while in suspension, or while cultured on plates. For the suspension, cells were collected in 1.5 ml tubes, and ultrasound was directly applied through the tube. For the anchored cells, ultrasound was applied on the bottom surface of the cell culture plate. The peptides were ultrasound for 5, 10 minutes with intensity of 1.1- 2.2 W/cm^2. The ultrasound increases the cellular uptake compared when applied in solution, while not much difference in uptake was observed when applied on the surface. (Figures 4.13, 4.14, 4.15).

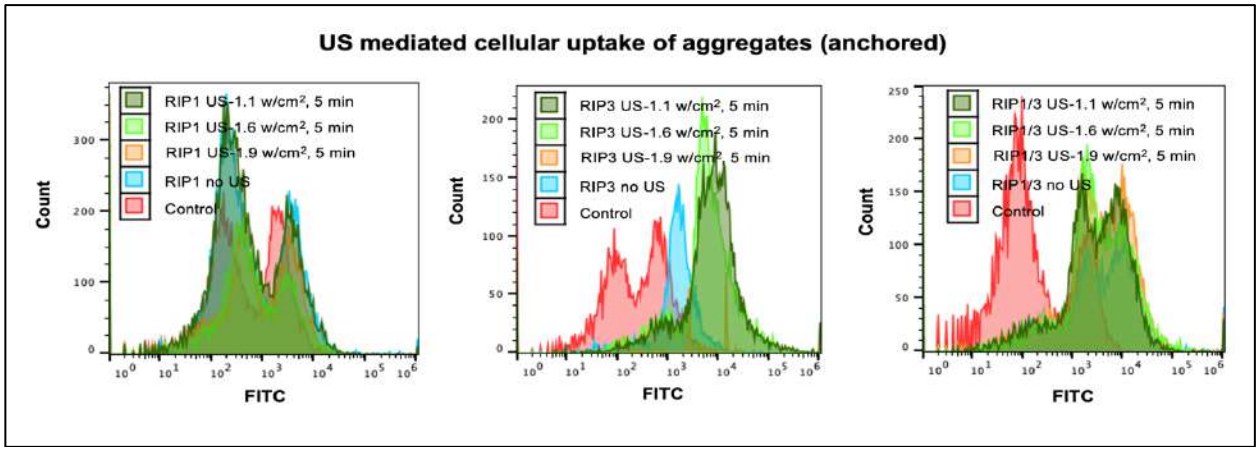

Figure 4.13 Ultrasound mediated peptide aggregates uptake anchored lower intensity.

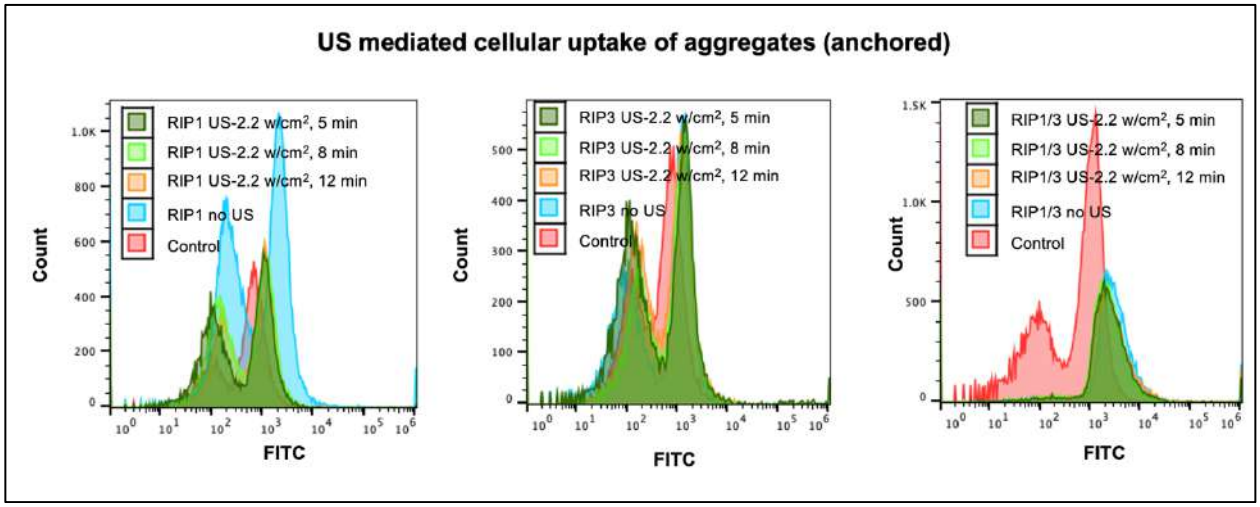

Figure 4.14 Ultrasound mediated peptide aggregates uptake anchored higher intensity.

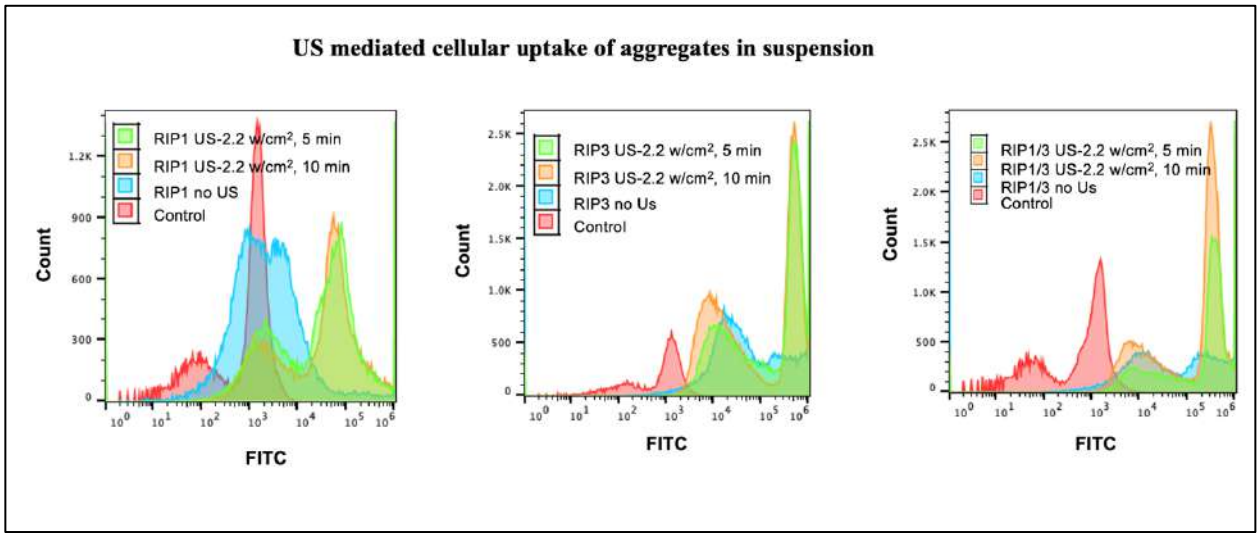

Figure 4.15 RIP1/RIP3 no ultrasound, and with ultrasound.

4.8. Uptake Mechanism

To determine whether the aggregates uptake is mediated by endocytosis mechanism, three endocytosis inhibitors were used, and measured the aggregates uptake. The inhibitors used were 5 µg/ ml or 10 µg/ ml of Chlorpromazine Hydrochloride (CPZ) which inhibits clathrin mediated endocytosis by preventing the assembly and disassembly of clathrin lattices on cells surface, 80 µM or 160 µM of Dynasore the Dynamin inhibitor which is essential for membrane fusion during endocytosis, and 25 µg/ml or 50 µg/ml of Cytochalasin D which inhibits actin polymerization and a phagocytosis inhibitor. The concentration of the inhibitors was doubled to check if it will affect the results. The measurement was performed by the Attune Nxt Flow Cytometer from Thermo Fisher Scientific in the laboratory. The cells were cultured in 24 wells plate at a density of 100,000 cells/500 µl/well. Then after 48 hours the inhibitors were added to the cells. 1 mM of the long sequence peptide RIP1-12 (TIYNSTGIQIGA), RIP3-12 (NIYNCSGVQVGD), and RIP1-12/RIP3-12 were prepared. After one day the peptides were labeled with NHS-Fluorescein. The cells were incubated for 90 minutes after inhibitor treatment, and subsequently treated with 100 µM peptide aggregates for 30 minutes. The results showed that the Dynasore, Chlorpromazine

Hydrochloride (CPZ) did not inhibit the uptake pathway for the peptides so the inhibition of cellular uptake of the peptide was by Cytochalasin D (Figures 4.16,4.17,4.18). Doubling the amount of concentration of the inhibitors did not affect the result.

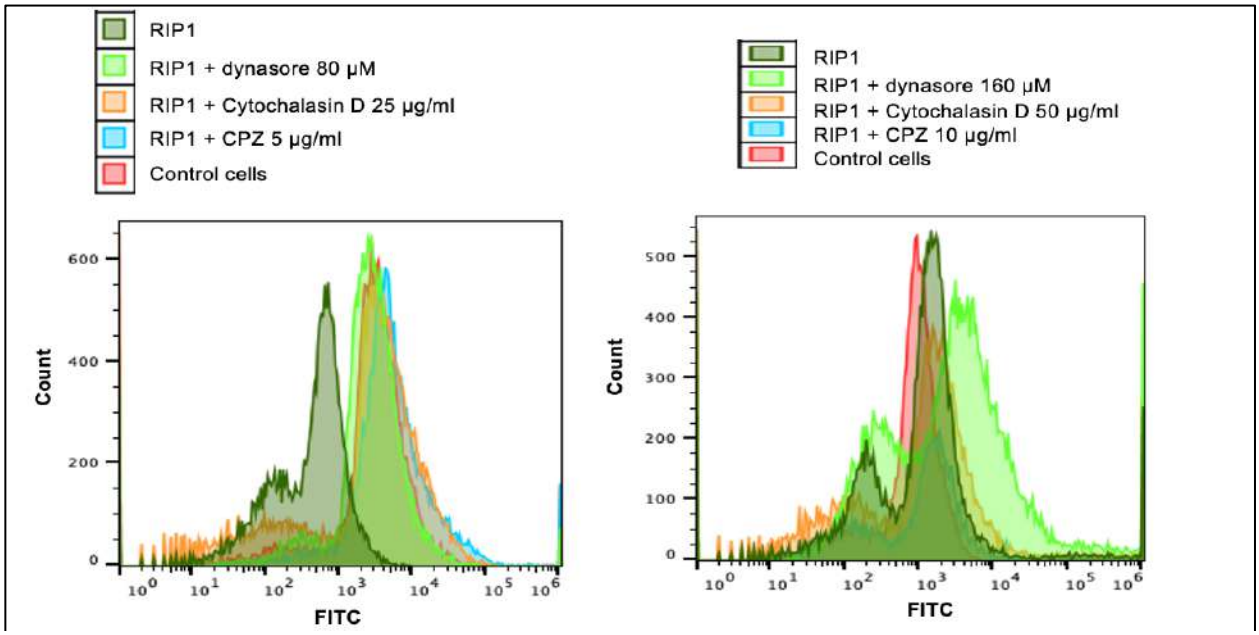

Figure 4.16 Cellular uptake of RIP1 in the presence of endocytosis inhibitors at two different concentrations.

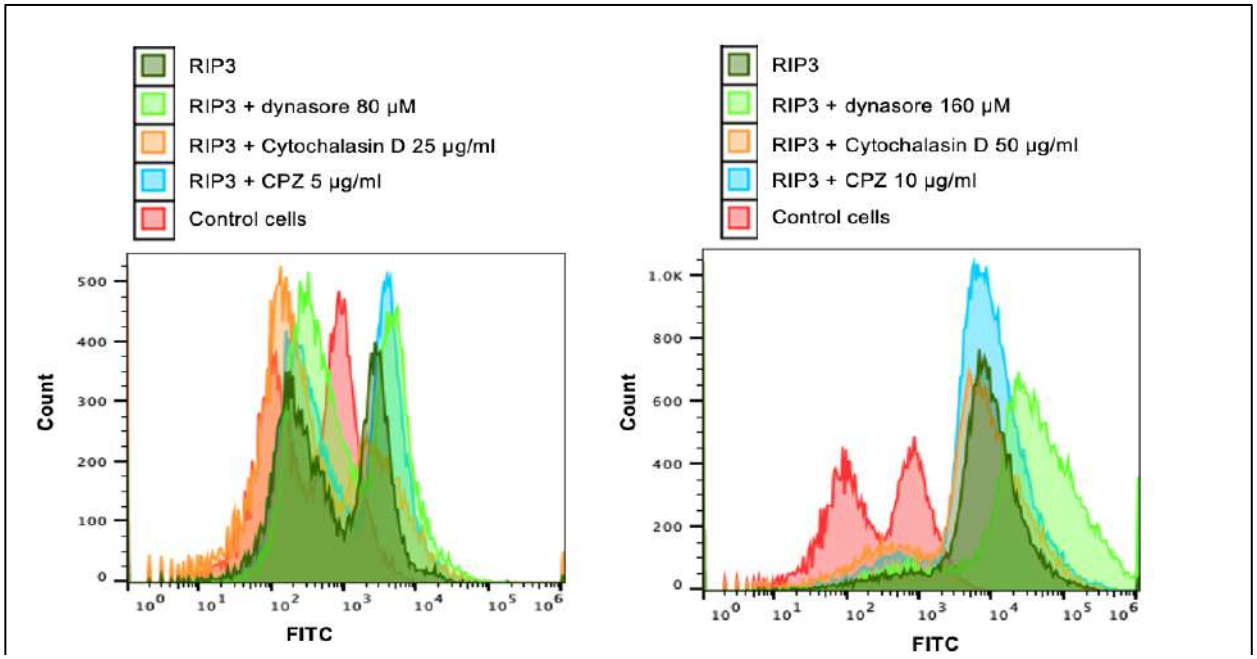

Figure 4.17 Cellular uptake of RIP3 in the presence of endocytosis inhibitors at two different concentrations.

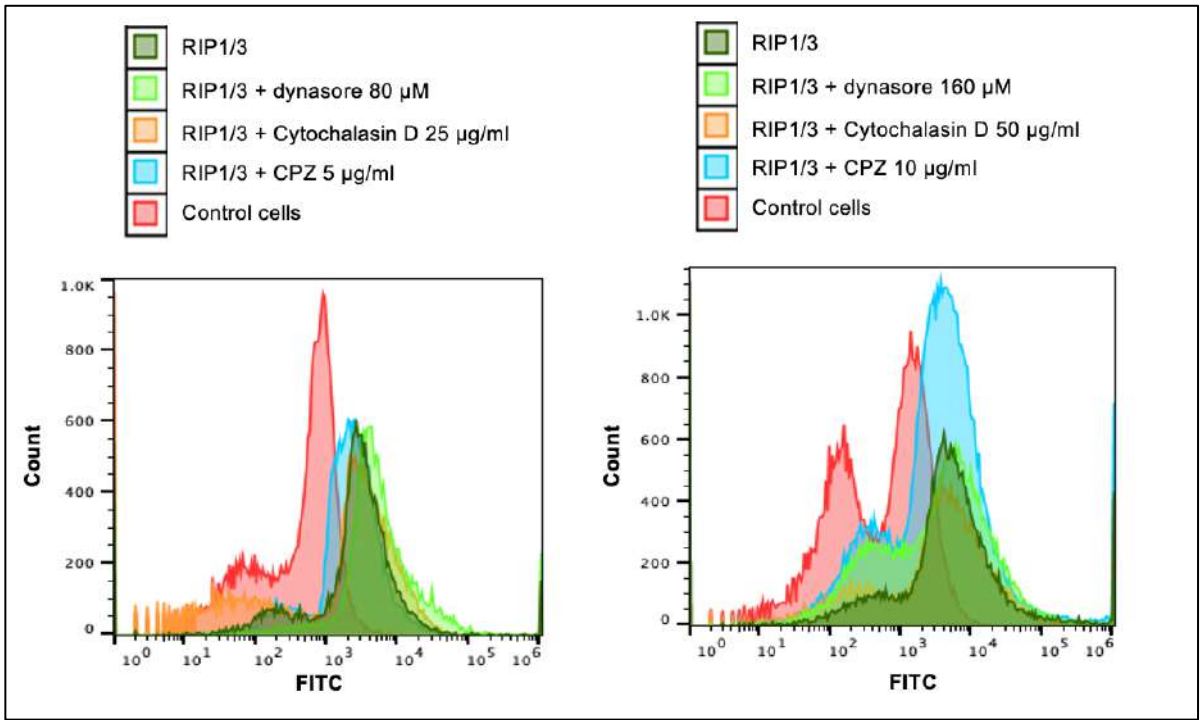

Figure 4.18 Cellular uptake of RIP1/3 in the presence of endocytosis inhibitors at two different concentrations.

4.9. Toxicity

To measure whether peptide aggregates induce cellular toxicity, alamarBlue assay was performed according to the manufactures protocol. The data showed no toxicity, moreover slightly higher cell viability compared to control cells (Figure 4.19). This may be due to the interference of the peptide aggregates with the resazurin dye, so the apoptosis/ necrosis assay was used to determine the toxicity study.

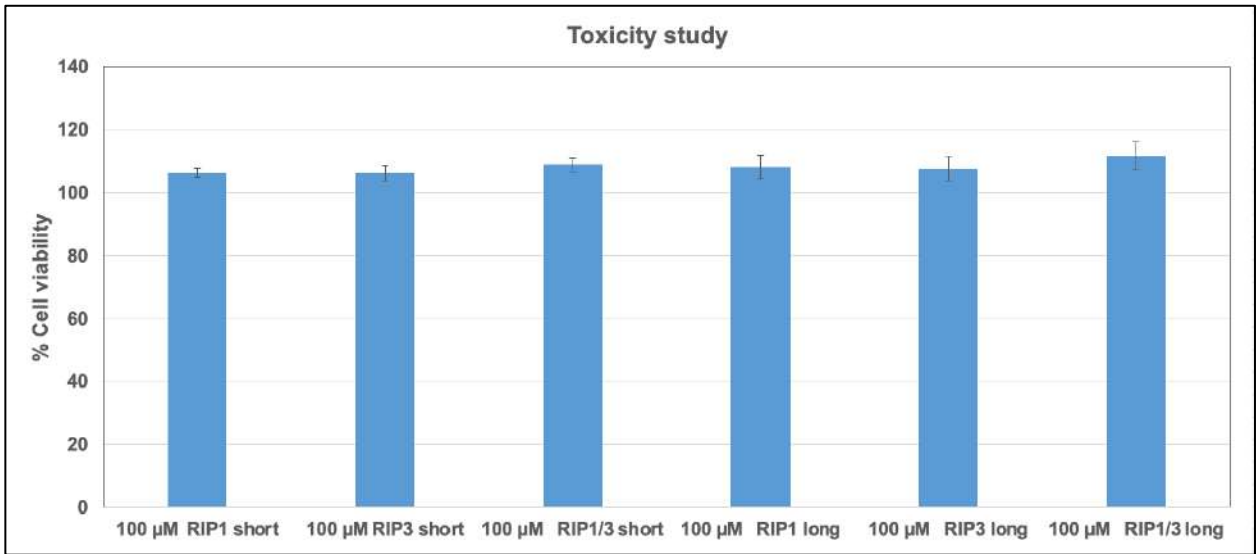

Figure 4.19 Alamar blue cell viability assay show no significant toxicity of both short and long peptides aggregates.

4.10. Apoptosis/ Necrosis

Apoptosis/ necrosis assay was used to detects toxicity event related to apoptosis and cell death due to necrosis. In particular, we studied whether peptide aggregates alone induced necrosis/apoptosis. The measurement was performed by the Attune Nxt Flow Cytometer from Thermo Fisher Scientific in the laboratory. Apoptosis and necrosis were assessed by PI/Annexin V staining using an apoptosis/necrosis kit from Biotium. Cisplatin was used as a model drug to assess peptide aggregates-based drug delivery to cancer cells. Representative flow cytometer data of the study is shown in (Figures 4.20,4.21,4.22,4.23). The analysis was shown in (Figures 4.24,4.25). The result showed that RIP1 peptide aggregates induce significant necrosis, while cisplatin (cis) at 10 µM induced significant apoptosis. Further no significant change in dead cell percentage was observed with cisplatin treatment, whereas peptide aggregates with and without cisplatin exhibited cell death.

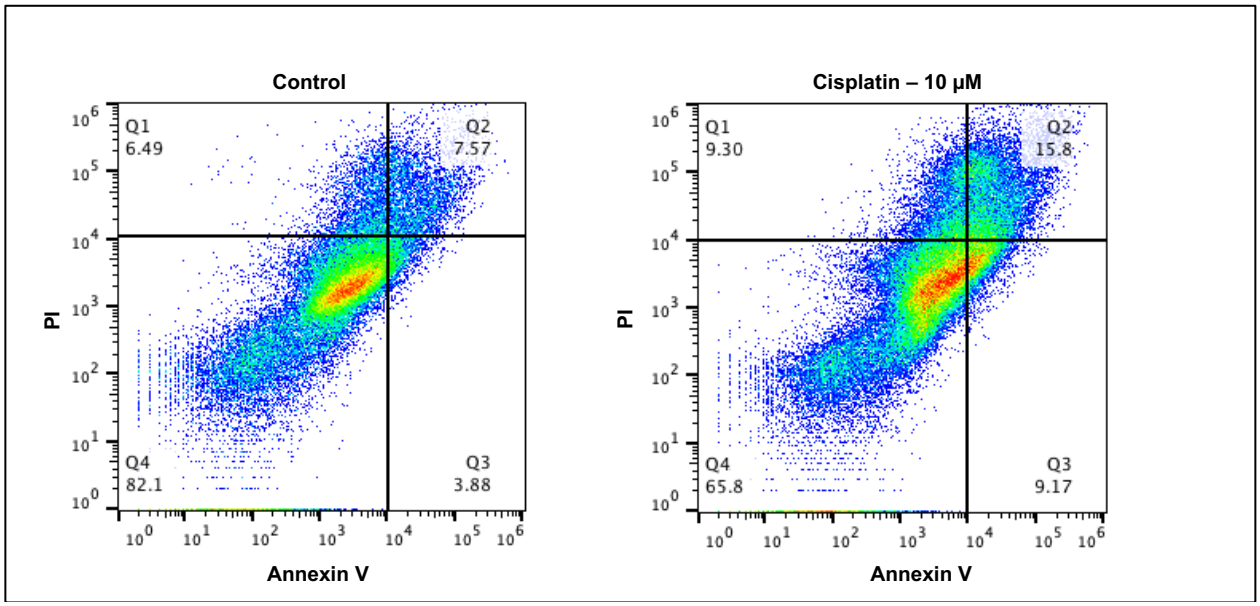

Figure 4.20 Annexin V/PI staining of cells with no treatment (control), and cells treated with cisplatin. Increased cell death and apoptosis can be seen in cisplatin treated cells, here, live cells (Q4), apoptotic cells (Q3), dead cells (Q2), and necrotic cells (Q1).

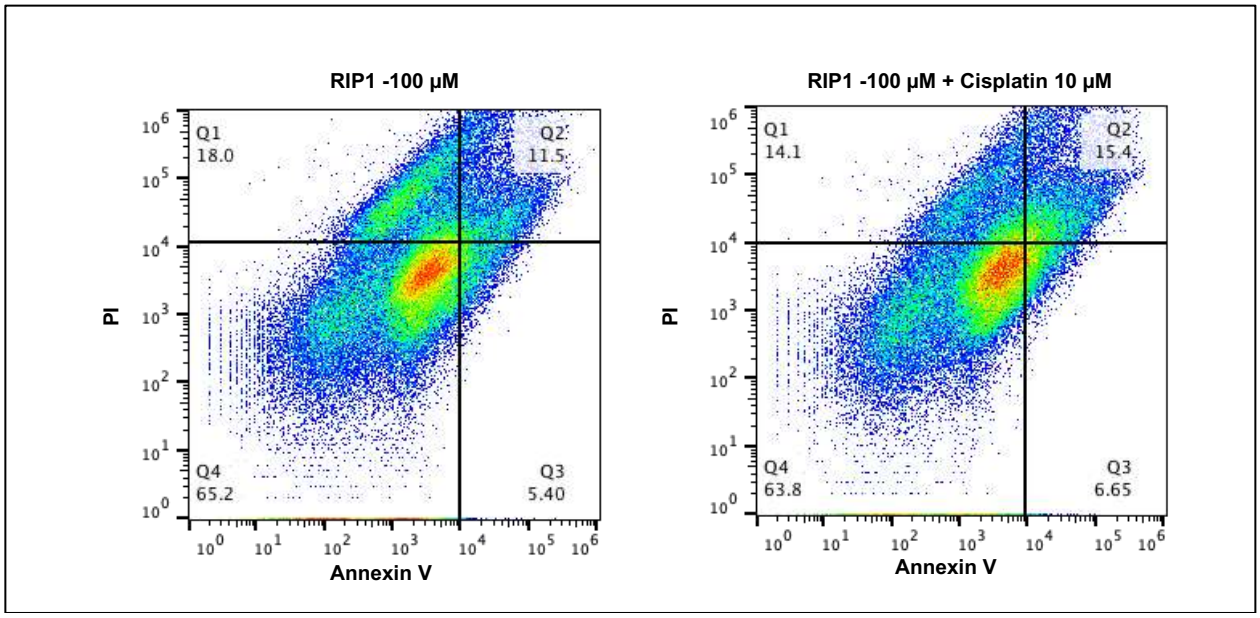

Figure 4.21 Annexin V/PI staining of cells with treated with RIP1, or RIP1 + cisplatin, live cells (Q4), apoptotic cells (Q3), dead cells (Q2), and necrotic cells (Q1).

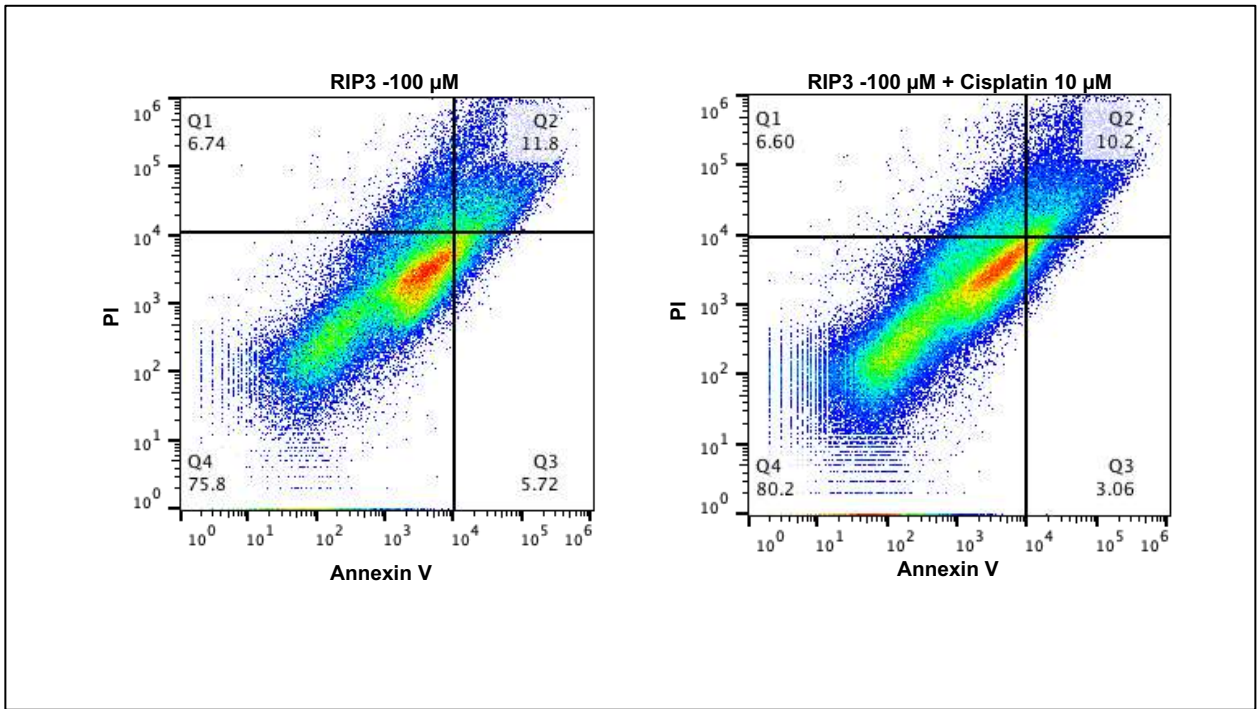

Figure 4.22 Annexin V/PI staining of cells with treated with RIP3, or RIP3 + cisplatin, live cells (Q4), apoptotic cells (Q3), dead cells (Q2), and necrotic cells (Q1).

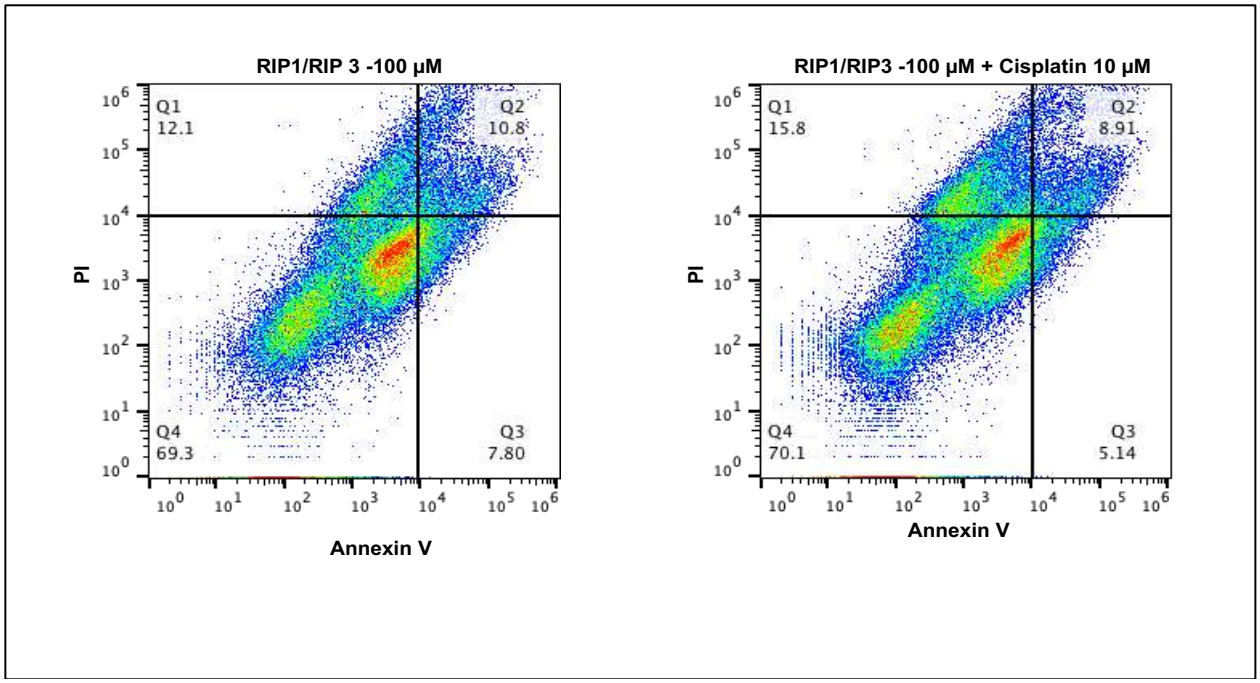

Figure 4.23 Annexin V/PI staining of cells with treated with RIP1/3, or RIP1/3 + cisplatin, live cells (Q4), apoptotic cells (Q3), dead cells (Q2), and necrotic cells (Q1).

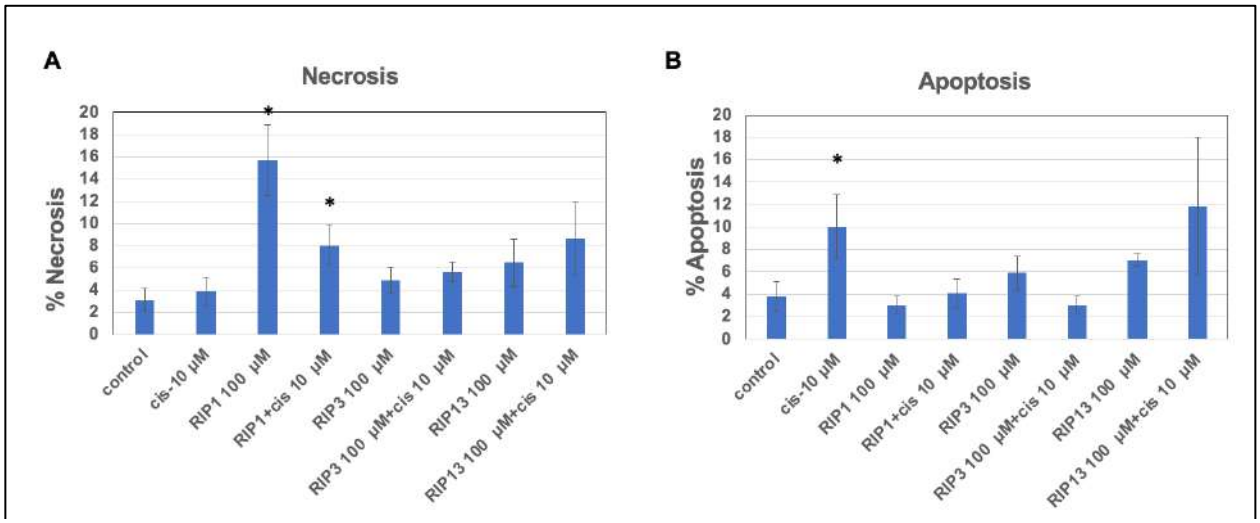

Figure 4.24 Annexin V/PI staining necrosis and apoptosis analysis. RIP1 treated cells showed significant necrosis compared to other treatment conditions. Cisplatin induced significant apoptosis compared to other treatment conditions. * $p < 0.05$.

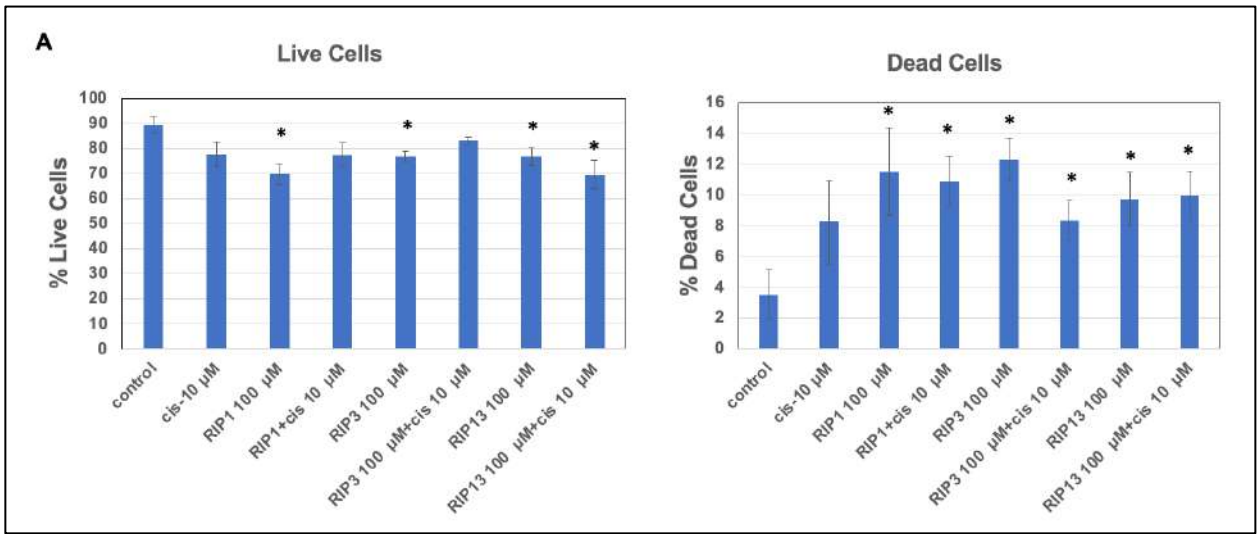

Figure 4.25 Annexin V/PI staining live cells and dead cells analysis. Peptide aggregates treated cells showed significant difference in live cells and dead cells percentage compared to control. Cisplatin showed no difference. * $p < 0.05$.

Chapter 5 : Discussion and Future Directions

5.1. Discussion and Future Directions

The thesis study reveals that the short 4 amino acid peptides RIP1-4 (IQIG), and RIP3-4 (VQVG) did not exhibit significant aggregation. On the other hand, peptides comprising 12 amino acids RIP1 (TIYNSTGIQIGA), and RIP3 (NIYNCSGVQVGD) showed aggregation properties at concentrations above 100 μM. The aggregation properties were confirmed by biochemical and biophysical characterization. Further, peptide aggregates showed ultrasound mediated mechano sensitive properties. The uptake of the aggregates was shown to be mediated by phagocytosis compared to endocytosis. In addition, the aggregates when applied to cancer cells at 100 μM, induced necrosis compared to apoptosis.

The results suggest that the longer the peptide sequence in the aggregation prone region, the easier it is to form aggregates in vitro. The smaller the peptide sequence, the higher concentration is needed to form aggregates. Further, the results show that the aggregates size would be tuned by ultrasound mediated breakage of the aggregates, which also improves the cellular uptake of the aggregates. The relatively larger size of the aggregates revealed by the DLS, and TEM images explain the phagocytosis mediated uptake mechanism compared to endocytosis. Regarding the aggregate's effects on cancer cells, the peptide aggregates induce necrosis. It may be due to just the peptide aggregates, not due to the RIP1/RIP3 peptide sequence.

This is the first time aggregation of short peptide sequences of RIP1/RIP3 has been studied. Previous studies were either focused on full protein or peptides with large number of amino acids covering the RHIM region [1,2,3,4]. Further applications of the peptide aggregates as drug depots were not explored before. Although peptide aggregation of RIP1/RIP3 has advantages compared to full length protein aggregation studies due to easier handling, and lower cost, the functional effects of the aggregates may be limited. RIP1/RIP3 peptide sequence only contain the aggregation prone region, but not the kinase domain of the protein, which is essential for the necroptosis function of the protein. Another limitation with peptides aggregates is the need of rather high concentration to form aggregation.

Studies still does not have a clear picture about the mechanism of RIP1 and RIP3 amyloid aggregates kinase activation, but it can be the beginning for further research about the amyloid structure and their role in biological functions and diseases. Hence, future studies should focus on investigation of both the full protein aggregation and small peptide sequences to have a clear understanding. In this thesis work a small segment of the RIP1, RIP3 proteins was examined, so for further research we will study more about the full proteins to understand the role of the RIP1/RIP3 protein aggregation in normal function and diseases. Further research on impact on cellular functions and immune response would yield important insights. In summary, the study covers approach for further research on investigating RIP1 and RIP3 peptides and proteins aggregation in vitro, in vivo, and potential applications in treating diseases.

5.2. References

[1] Liu, Y., Liu, T., Lei, T., Zhang, D., Du, S., Girani, L., Qi, D., Lin, C., Tong, R., & Wang, Y. (2019). RIP1/RIP3-Regulated Necroptosis as a Target for Multifaceted DiseaseTherapy (Review). *International Journal of Molecular Medicine, 44*, 771-786.

[2] Moquin, D., & Chan, F.K. (2010). The molecular regulation of programmed necrotic cell injury. *Trends Biochem. Sci.,* 35,434-441.

[3]Wu, X.-N., Yang, Z.-H., Wang, X.-K., Zhang, Y., Wan, H., Song, Y., Chen, X., Shao, J., & Han, J. (2014, November). Distinct roles of Rip1-Rip3 hetero- and Rip3-Rip3 homo-interaction in mediating necroptosis. *Cell death and differentiation,21*(11),1709-1720.

[4] Sun, L., Wang, H., Wang, Z., He, S., Chen, S., Liao, D., Wang, L., Yan, J., Liu, W., Lei, X., & Wang, X. (2012, January 19). Mixed lineage kinase domain-like protein mediates necrosis signaling downstream of rip3 kinase. *Cell, 148*(1-2), 213-227.